Available online at www.sciencedirect.com
ScienceDirect
Geochimica et Cosmochimica Acta 75 (2011) 825–843
Geochimica et Cosmochimica Acta
www.elsevier.com/locate/gca

Submarine groundwater discharge is an important net source of light and middle REEs to coastal waters of the Indian River Lagoon, Florida, USA

Karen H. Johannesson [a,*], Darren A. Chevis [a], David J. Burdige [b], Jaye E. Cable [c], Jonathan B. Martin [d], Moutusi Roy [d,1]

[a] Department of Earth and Environmental Sciences, Tulane University, New Orleans, LA 70118, USA
[b] Department of Ocean, Earth, and Atmospheric Science, Old Dominion University, Norfolk, VA 23529, USA
[c] Department of Oceanography and Coastal Sciences, Louisiana State University, Baton Rouge, LA 70803, USA
[d] Department of Geological Sciences, University of Florida, Gainesville, FL 32611, USA

Received 30 July 2010; accepted in revised form 30 October 2010; available online 13 November 2010

Abstract

Porewater (i.e., groundwater) samples were collected from multi-level piezometers across the freshwater–saltwater seepage face within the Indian River Lagoon subterranean estuary along Florida's (USA) Atlantic coast for analysis of the rare earth elements (REE). Surface water samples for REE analysis were also collected from the water column of the Indian River Lagoon as well as two local rivers (Eau Gallie River, Crane Creek) that flow into the lagoon within the study area. Concentrations of REEs in porewaters from the subterranean estuary are 10–100 times higher than typical seawater values (e.g., Nd ranges from 217 to 2409 pmol kg^{-1}), with submarine groundwater discharge (SGD) at the freshwater–saltwater seepage face exhibiting the highest REE concentrations. The elevated REE concentrations for SGD at the seepage face are too high to be the result of simple, binary mixing between a seawater end-member and local terrestrial SGD. Instead, the high REE concentrations indicate that geochemical reactions occurring within the subterranean estuary contribute substantially to the REE cycle. A simple mass balance model is used to investigate the cycling of REEs in the Indian River Lagoon and its underlying subterranean estuary. Mass balance modeling reveals that the Indian River Lagoon is approximately at steady-state with respect to the REE fluxes into and out of the lagoon. However, the subterranean estuary is not at steady-state with respect to the REE fluxes. Specifically, the model suggests that the SGD Nd flux, for example, exported from the subterranean estuary to the overlying lagoon waters exceeds the combined input to the subterranean estuary from terrestrial SGD and recirculating marine SGD by, on average, ~100 mmol day^{-1}. The mass balance model also reveals that the subterranean estuary is a net source of light REEs (LREE) and middle REEs (MREE) to the overlying lagoon waters, but acts as a sink for the heavy REEs (HREE). Geochemical modeling and statistical analysis further suggests that this fractionation occurs, in part, due to the coupling between REE cycling and iron redox cycling within the Indian River Lagoon subterranean estuary. The net SGD flux of Nd to the Indian River Lagoon is ~7-fold larger than the local effective river flux to these coastal waters. This previously unrecognized source of Nd to the coastal ocean could conceivably be important to the global oceanic Nd budget, and help to resolve the oceanic "Nd paradox" by accounting for a substantial fraction of the hypothesized missing Nd flux to the ocean.

* Corresponding author. Address: Department of Earth and Environmental Sciences, Tulane University, 6823 St. Charles Avenue, Blessey Hall, New Orleans, LA 70118-5698, USA. Tel.: +1 504 862 3193; fax: +1 504 865 5199.
E-mail address: kjohanne@tulane.edu (K.H. Johannesson).
[1] Present address: Department of Chemical Oceanography, College of Oceanic and Atmospheric Sciences, Oregon State University, Corvallis, OR 97331, USA.

0016-7037/$ - see front matter © 2010 Elsevier Ltd. All rights reserved.
doi:10.1016/j.gca.2010.11.005

1. INTRODUCTION

Understanding the sources and sinks of trace elements such as the rare earth elements (REE) in the oceans has important implications for quantifying their global geochemical cycles, their application as paleoceanographic tracers, and in discerning the geochemical reactions that mobilize, sequester, and fractionate REEs in the environment. This is especially important for neodymium (Nd) as radiogenic Nd isotopes are commonly used in paleoceanographic investigations over glacial–interglacial to million year time scales (e.g., von Blanckenburg, 1999; Rutberg et al., 2000; Frank, 2002; Scher and Martin, 2004; Piotrowski et al., 2005; Frank et al., 2006; Foster et al., 2007; MacLeod et al., 2008; Pahnke et al., 2008).

However, our ability to confidently use Nd isotopes to trace oceanic water mass circulation in the modern ocean as well as in paleoceanographic studies is hampered, in part, by the relatively poor constraints on the sources and sinks of Nd to and from the global ocean (von Blanckenburg, 1999; Lacan and Jeandel, 2001; Frank, 2002; Goldstein and Hemming, 2003; Piotrowski et al., 2008; also see Johannesson and Burdige, 2007, for a general review of this problem). Related to this is the so-called "Nd paradox" (Bertram and Elderfield, 1993; Jeandel et al., 1995, 1998; Tachikawa et al., 1997, 1999a,b; Lacan and Jeandel, 2001; Goldstein and Hemming, 2003; Siddall et al., 2008; Arsouze et al., 2009), which is the apparent decoupling of dissolved Nd concentrations (nutrient-like water column profiles suggestive of vertical cycling and relatively long, $\sim 10^4$ years, oceanic residence times) and Nd isotope ratios (inter- and intra-ocean differences, which presumably exclude vertical cycling and supports an oceanic residence time of Nd that must be similar to, or less than the ~500–1500 years oceanic mixing time).

More specifically, estimates of the atmospheric and riverine fluxes, which are considered the chief sources of Nd to the ocean, are insufficient by roughly a factor of 10 to balance the oceanic Nd budget and preserve the observed inter- and intra-oceanic Nd isotope values. The difference, which amounts to $\sim 5.6 \times 10^7$ moles of Nd per year, is known as the "missing Nd flux" and has been the subject of substantial speculation (Tachikawa et al., 2003; Lacan and Jeandel, 2005a; Arsouze et al., 2009). However, other than the broadly defined "boundary exchange" occurring along continental margins (e.g., Lacan and Jeandel, 2005b), none of the other specific processes discussed in the literature – redissolution of particulate- or sediment-associated Nd in mid- to high-salinity regions of estuaries (Sholkovitz and Szymczak, 2000), diffusive fluxes of porewater REEs to the overlying water column (Elderfield and Sholkovitz, 1987), or dissolution of atmospheric particle derived Nd (i.e., the atmospheric Nd flux) in the oceans (Zhang et al., 2008; Arsouze et al., 2009) – appear to have the proper magnitude and Nd isotope values to balance the ocean Nd budget.

Using average Nd concentrations and isotope values for groundwaters from the literature, and an estimate of the global, terrestrial submarine groundwater discharge (SGD) flux, Johannesson and Burdige (2007) speculated that SGD may constitute an important component of this missing Nd flux. However, Johannesson and Burdige (2007) did not measure Nd in actual SGD samples and only hypothesized that the marine component of the SGD Nd flux may be considerable. Submarine groundwater discharge includes all flow of water from the seafloor into the overlying marine water column within continental margin settings notwithstanding the physical driving mechanism and chemical composition (Church, 1996; Burnett et al., 2003; Moore, 2010). Consequently, SGD consist of both "fresh submarine groundwater discharge" originating from meteoric recharge of terrestrial aquifers and "recirculated saline submarine groundwater discharge" (i.e., marine waters) that cycles through coastal aquifers due to processes such as tidal pumping, wave set-up, bioirrigation, and/or geothermal or density gradients (Taniguchi et al., 2002). Hereafter, these components of SGD are referred to as "terrestrial SGD" and "marine SGD", respectively, and the combination of the two as "total SGD" (Martin et al., 2007).

A number of previous studies have shown that SGD represents a significant flux of water, nutrients, carbon, and metals to the oceans (Moore, 1996, 1997, 2010; Cai et al., 2003; Charette and Buesseler, 2004; Slomp and Van Cappellen, 2004; Kim et al., 2005; Windom et al., 2006; Charette, 2007; Moore et al., 2008). In this contribution, we present REE concentration data for porewaters (i.e., groundwaters) and surface waters of the Indian River Lagoon system, and show using a simple mass balance approach that, to a first approximation, total SGD is a substantial net source of light REEs (LREE) and middle REEs (MREE) to these coastal waters.

2. STUDY SITE

The field site is located along the Indian River Lagoon near the city of Melbourne, Florida (Fig. 1). The Indian River Lagoon system occupies a large portion of Florida's Atlantic coast, extending for 250 km, and includes the Mosquito and Banana River Lagoons to the north. The lagoon is characterized as microtidal as the amplitudes of tides are typically less than 10 cm. Nonetheless, the shallow water column (mean depth of 1.5 m, with a maximum depth of 5 m) is generally well mixed owing to changes in water level largely driven by wind.

Pleistocene beach ridges surround the Indian River Lagoon in the study site. The lagoon is underlain by the Holocene Anastasia Formation, which makes up the Surficial Aquifer in the study area. The Anastasia Formation consists of quartz sand that is interbedded with coquina, along with minor amounts of silt, clay, and carbonate rock fragments (Martin et al., 2007). Porosity of the Surficial Aquifer within the Indian River Lagoon subterranean estuary (Moore, 1999) ranges from 37% to 45%, whereas the hydraulic conductivity ranges between 10^{-4} and 10^{-10} m s^{-1} within the upper 300 cm, but exhibits a more uniform range of 10^{-4}–10^{-8} m s^{-1} in the top 70 cm (Martin et al., 2004; Hartl, 2006; Smith et al., 2008a; Roy et al., 2010). The Surficial Aquifer is separated from the underlying Floridan Aquifer system (Paleocene to Oligocene

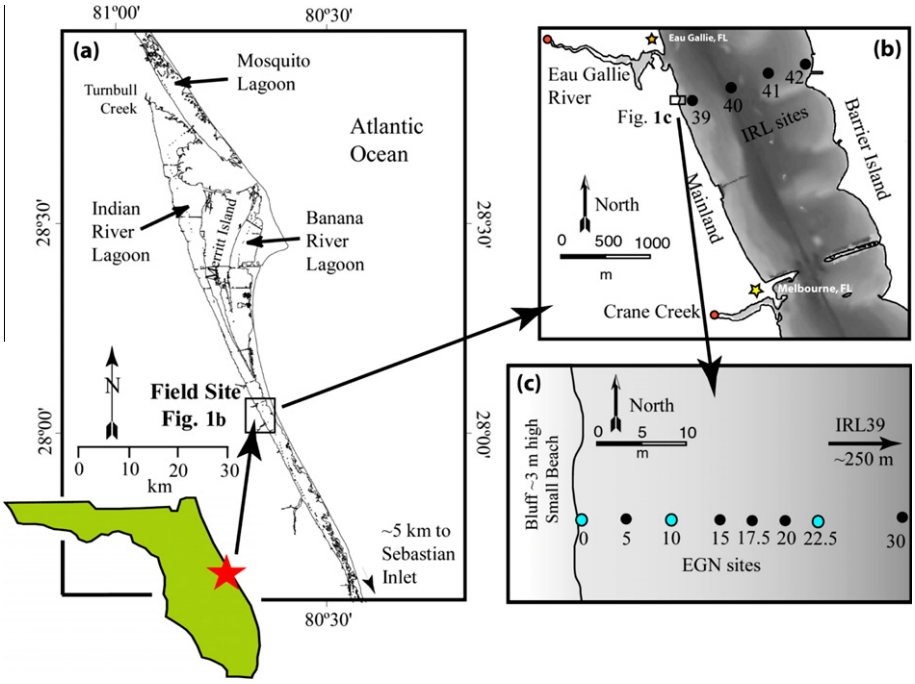

Fig. 1. Location of the field site within the Indian River Lagoon system is shown in panel (a), whereas panel (b) illustrates the immediate vicinity of the field site, including the portion of the Indian River Lagoon considered in the mass balance model (i.e., portion of the lagoon bounded on the north by the Eau Gallie River, the south by Crane Creek, the east by the barrier island, and the west by the mainland). Sampling locations for the Eau Gallie River and Crane Creek are shown as small red circles on panel (b). Location of Melbourne, FL and Eau Gallie, FL are shown as yellow and orange stars, respectively on panel (b). Panel (c) presents a map showing the distribution of multi-level piezometers (multisamplers; Martin et al., 2003) installed offshore and into the Indian River Lagoon. Multisamplers EGN-0, EGN-10, and EGN-22.5 were sampled for REEs in this study. Map is modified from Martin et al. (2007). Multisampler CIRL-39, which was not sampled for REEs, but discussed in the text, is located 250 m offshore. (For interpretation of the references to color in this figure legend, the reader is referred to the web version of this article.)

limestones) by approximately 30 m of the confining Hawthorne Group (Miocene sand, marl, clay, limestone, dolostone, and phosphatic materials; Miller, 1986). The thickness of the Hawthorne Group rocks in the study region indicates that essentially all of the terrestrial SGD to the Indian River Lagoon subterranean estuary originates within the Surficial Aquifer (Martin et al., 2007).

Our study specifically focuses on a portion of the Indian River Lagoon that is located ~4.5 km north of Melbourne, Florida, and ~0.5 km south of Eau Gallie, Florida (Fig. 1b and c). Freshwater is delivered to the studied portion of the Indian River Lagoon via direct precipitation, urban runoff, discharge of the Eau Gallie River and Crane Creek, and terrestrial SGD (Martin et al., 2007). Fluxes of SGD were previously determined at the study site using a combination of methods that included seepage meters, chemical and thermal tracers, and models of chemical profiles (excess ^{222}Rn, Ra isotope decay, Cl concentrations; Cable et al., 2004, 2006; Martin et al., 2004, 2006, 2007; Smith et al., 2008a,b; Roy et al., 2010). The flux of terrestrial SGD decreases with distance offshore becoming negligible near the freshwater–saltwater seepage face within the subterranean estuary (Fig. 2). Here, recirculated marine SGD mixes with terrestrial SGD and the combined flux (i.e., total SGD) discharges to the overlying lagoon waters along the freshwater–saltwater seepage face. Marine SGD accounts for more than 90% of the total SGD to the Indian River Lagoon, and this flux is largely driven by bioirrigation (Cable et al., 2006; Martin et al., 2006, 2007; Roy et al., 2010). The depth of bioirrigation (i.e., active and/or passive flushing of bottom water through sediments resulting from activities of benthic macrofauna; Burdige, 2006) increases from ~10 cm at the shoreline to approximately 40 cm at the freshwater–saltwater seepage face (Fig. 2; Smith et al., 2008a; Roy et al., 2010). Further offshore beyond the freshwater–saltwater seepage face (e.g., in the vicinity of CIRL-39, 250 m offshore), bioirrigation results in rapid, daily exchange of lagoon waters with porewaters within the upper 70 cm of the sediments, leading to flow rates as large as 150 cm day^{-1} (Martin et al., 2004, 2006). Consequently, marine SGD is chiefly Indian River Lagoon water that is cycled through the lagoon bottom sediments by bioirrigation, whereas the total SGD consists of both a relatively small component of terrestrial SGD and this substantially larger component (~2 orders of magnitude larger) of marine SGD (Cable et al., 2004; Martin et al., 2004, 2006, 2007; Fig. 2). Exchange of Indian River Lagoon waters with the ocean occur via three inlets located within the southern part of the lagoon. Consequently, the residence time of water in the Indian River Lagoon can be as much as a year in the far north, but is generally on the order of 18 days in the vicinity of the study site (Smith, 1993).

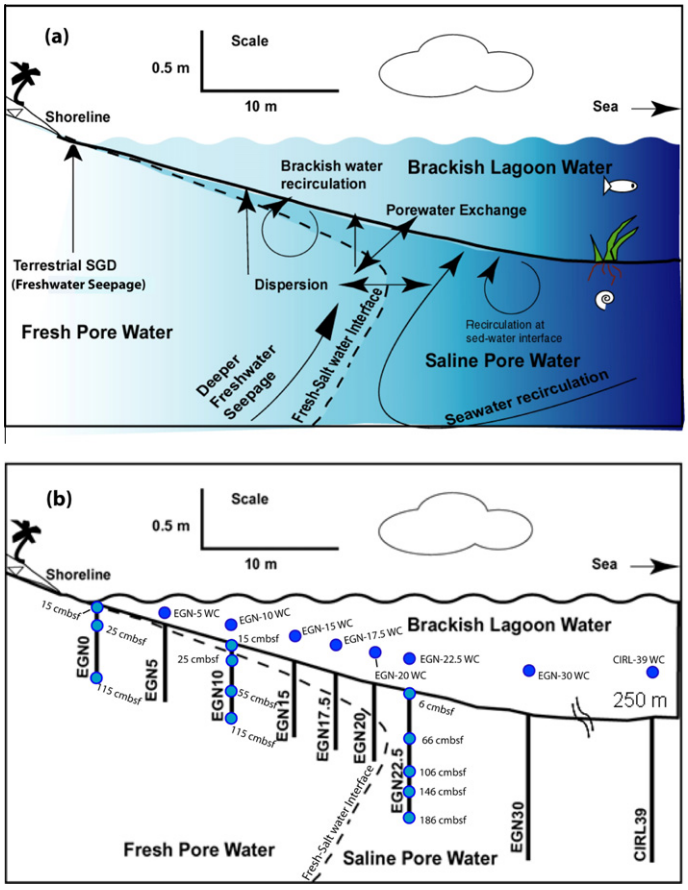

Fig. 2. Schematic cross-section through the studied portion of the Indian River Lagoon along the near-shore multisampler transect shown in Fig. 1c. Panel (a) illustrates hypothetical flow paths for SGD in the subterranean estuary underlying the Indian River Lagoon study site. Note, "sed–water interface" indicates the sediment–water interface. Approximate locations of the multisamplers installed in the study area and the locations where porewater and surface water samples were collected are shown in panel (b), where cmbsf = centimeters below sea floor. Specifically, blue circles superimposed on multisamplers EGN-0, EGN-10, and EGN-22.5 depict the approximate depths below the seafloor where porewater samples were collected for REE analysis. The darker blue circles in the overlying lagoon water column show the approximate locations where water column samples were collected. The cross sections are modified after Martin et al. (2005), Cable et al. (2007), Roy (2009), and Roy et al. (2010). Note that multisampler ENG-22.5 occurs within the mixing zone (i.e., subterranean estuary) between fresh, terrestrial SGD and saline, marine SGD. (For interpretation of the references to color in this figure legend, the reader is referred to the web version of this article.)

Sediments within the Indian River Lagoon subterranean estuary are described in detail in Hartl (2006) and Roy et al. (2010). Four sediment cores recovered in the vicinity of CIRL-39 (Figs. 1 and 2) consisted of 2 m of black (sulfide-rich), marine sediments overlying orange, Fe(III) oxide/oxyhydroxide coated quartz sands of terrestrial origin (Hartl, 2006). The thickness of the orange sediments is currently unknown as they extended to the base of these sediment cores. Roy et al. (2010) report similar lithostratigraphy for 6 cores collected along the nearshore transect shown in Fig. 1c. Specifically, these sediment cores were collected approximately 1 m north of sites EGN-0, EGN-10, EGN-20, EGN-22.5, EGN-30, and CIRL-39 (Fig. 1c; Roy et al., 2010). The thickness of the black, sulfide-rich marine sediments is ~17 cm at the shoreline (EGN-0), but increases in thickness with distance from shore, reaching 68 cm at EGN-30, and more than 250 cm at CIRL-39 (Hartl, 2006; Roy et al., 2010). Because sedimentation rates vary little within the Indian River Lagoon (Hartl, 2006), the increase in the thickness of the sulfide-rich marine sediments with distance offshore is interpreted to be the result of sea-level rise and the consequent increase in Fe–sulfide accumulation times accommodated by progressive seawater inundation (Roy et al., 2010).

3. METHODS

3.1. Sample collection

Methods employed to determine volumetric fluxes of SGD that are used here in the mass balance model were previously described (Cable et al., 2004; Martin et al., 2004, 2006, 2007). Porewater (i.e., groundwater) samples for REE analysis were collected in April 2007 from three multilevel piezometers (i.e., multisamplers; Martin et al., 2003) along a near-shore transect that extends 30 m from

the Indian River Lagoon mainland shore (i.e., 0 m; Fig. 1c) by pumping water from the different multisampler ports into an overflow cup using a peristaltic pump (Martin et al., 2007; Roy et al., 2010). Before porewater samples were collected, the specific conductivity, dissolved oxygen, temperature, and salinity of pumped waters was monitored until these parameters stabilized. In each case, less than 2 L was pumped in order to minimize the possibility of induced vertical flow during sampling. Once these parameters stabilized, porewater (~60–100 mL) was collected (via pumping) and subsequently filtered through 0.45 μm in-line (GEOTECH, polyether sulfone membrane) filter cartridges directly into precleaned (acid washed) HDPE sample bottles. Sample bottles were rinsed three times with the filtered porewater before filling. The filtered porewater samples were immediately acidified with ultra-pure HNO_3 (Seastar Chemical, Baseline, sub-boiling, distilled in quartz) to pH < 2. Samples for major cations (Ca^{2+}, Mg^{2+}, Na^+, K^+) were preserved with a drop of ultra-pure HNO_3, whereas aliquots for Cl^- and SO_4^{2-} analysis were not acidified. Samples of the Indian River Lagoon water column were collected identically in April 2007. Freshwater endmembers of the Eau Gallie River and Crane Creek (i.e., salinity = 0‰; Fig. 1b) were collected in late March 2009 using a similar approach (i.e., see Johannesson et al., 2004) that employed 0.45 μm in-line (Gelman Science, polyether sulfone membrane) filter capsules followed by immediate acidification with ultra-pure HNO_3 (Seastar Chemical, Baseline).

3.2. Sample analysis

Major solutes (Ca^{2+}, Mg^{2+}, Na^+, K^+, Cl^-, SO_4^{2-}) were determined in waters from the Indian River Lagoon system by ion chromatography (Dionex DX500) at the University of Florida. Alkalinity was determined by standard titration methods. Chloride was measured in the Eau Gallie River and Crane Creek samples at Tulane University using a Fisher Scientific Accumet® XL50 dual channel pH, ion, conductivity meter with an Accumet® chloride electrode (13-620-627). Dissolved Fe concentrations were determined by high-resolution (magnetic sector) inductively coupled plasma mass spectrometry (HR-ICP-MS, Finnigan MAT Element II) at the University of Florida by monitoring ^{56}Fe (Roy et al., 2010). Samples were diluted 50-fold with 5% (v/v) ultra-pure HNO_3, and spiked with rhodium as an internal standard (Roy et al., 2010). Dissolved Fe concentrations were quantified using in-house, gravimetrically prepared standards, with the analytical accuracy and precision evaluated by analyzing the National Research Council Canada (Ottawa, Ontario, Canada) Standard Reference Materials for seawater (NASS-5) and river water (SLRS-4; see Roy et al., 2010, for details).

Acidified samples (50 mL) for REE analysis were first loaded onto Poly-Prep columns (Bio-Rad Laboratories) packed with AG 50 W-X8 (100–200 mesh, hydrogen form, Bio-Rad Laboratories) cation-exchange resin at approximately 1 mL min^{-1} in order to separate the REEs from the major salts (e.g., Elderfield and Greaves, 1983; Greaves et al., 1989; Klinkhammer et al., 1994; Johannesson et al., 2005). Iron and Ba were subsequently eluted from the columns using 1.75 M ultra-pure HCl (Seastar Chemicals, Baseline, sub-boiling, distilled in quartz) and 2 M ultra-pure HNO_3 (Seastar Chemicals, Baseline), respectively. The REEs were then eluted from the columns using 8 M ultra-pure HNO_3 (Seastar Chemicals, Baseline, sub-boiling, distilled in quartz) and collected in Teflon® beakers. The eluant was subsequently taken to dryness on a hot-plate, and the residue then redissolved in 10 mL of a 1% v/v ultra-pure HNO_3 solution. Each 10 mL sample was then spiked with ^{115}In as an internal standard and analyzed for the REEs by HR-ICP-MS (Finnigan MAT Element II) at Tulane University. We monitored ^{139}La, ^{140}Ce, ^{141}Pr, ^{143}Nd, ^{145}Nd, ^{146}Nd, ^{147}Sm, ^{149}Sm, ^{151}Eu, ^{153}Eu, ^{155}Gd, ^{157}Gd, ^{158}Gd, ^{159}Tb, ^{161}Dy, ^{163}Dy, ^{165}Ho, ^{166}Er, ^{167}Er, ^{169}Tm, ^{172}Yb, ^{173}Yb, and ^{175}Lu (low- and medium-resolution mode) as many of these isotopes are free of isobaric interferences, and because monitoring more than one isotope of a given element provides an additional check for potential interferences. In addition, the Eu isotopes and the heavy REEs (HREE) where also monitored in high-resolution mode, which allowed us to resolve interferences on ^{151}Eu and ^{153}Eu from BaO^+ species formed in the plasma stream, and $LREEO^+$ and middle $REEO^+$ ($MREEO^+$) species on the HREEs. The HR-ICP-MS was calibrated and the concentrations of REEs in the samples confirmed with a series of REE calibration standards of known concentrations (1, 2, 5, 10, 100, 500, and 1000 ng kg^{-1}). The calibration standards were prepared from NIST traceable High Purity Standards (Charleston, SC). In addition, check standards for the REEs were prepared using Perkin–Elmer multi-element solutions. The National Research Council Canada (Ottawa, Ontario, Canada) Standard Reference Material (SRM) for estuarine waters (SLEW-3) was analyzed to check for accuracy by comparison to the measured REE values for SLEW-3 reported by Lawrence and Kamber (2007). Analytical precision of the REE analyses was always better than 4% relative standard deviation (RSD), and generally better than 2% RSD.

3.3. REE solution complexation modeling

Waters from the Indian River Lagoon system range in concentration from dilute freshwaters that characterize the terrestrial component of SGD and the inflow streams to the saline waters of the lagoon itself (salinity of lagoon water near our field site ranges from 22‰ to 29‰; Martin et al., 2007). Consequently, solution complexation of the REEs in waters from the Indian River Lagoon system was evaluated using a combined specific ion interaction and ion pairing model initially developed for the REEs by Millero (1992). The model links the specific ion interaction approach (e.g., Pitzer, 1979) with and ion pairing model (Garrels and Thompson, 1962; Millero and Schreiber, 1982), thus allowing for the evaluation of REE complexation with inorganic ligands in dilute to highly saline natural waters (Johannesson and Lyons, 1994; Johannesson et al., 1996a,b). The model was updated by adding the most recently determined stability constants for REEs complexation with inorganic ligands (e.g., Lee and Byrne, 1992; Schijf and Byrne, 1999, 2004; Klungness and Byrne, 2000;

Luo and Byrne, 2001, 2004). Free concentrations of inorganic ligands (e.g., $[CO_3^{2-}]_F$, $[SO_4^{2-}]_F$) used in the REE complexation modeling were computed from the major solute composition of Indian River Lagoon waters via the SpecE8 program of the Geochemist's Workbench® (release 7.0; Bethke, 2008) using the thermodynamic data base from PHRQPITZ (Plummer et al., 1989), and following the approach outlined by Millero and Schreiber (1982).

3.4. Mass balance model

Mass balance calculations were performed using a standard box model approach, which assumes steady-state flow conditions and includes separate boxes (i.e., reservoirs) for: (1) the water column portion of the Indian River Lagoon system; (2) the subterranean estuary beneath the lagoon; and (3) the coastal ocean (Fig. 3). The section of the Indian River Lagoon considered in the box model is shown in Fig. 1b, and includes the portion of the Indian River Lagoon between the Eau Gallie River and Crane Creek. Because the distance between the Eau Gallie River and Crane Creek is 5 km, the width of the Indian River Lagoon in the study region (i.e., distance from the mainland to the barrier island) is 1.8 km, and the average depth of the lagoon is 1.5 m, the volume of the lagoon considered in our model is 1.35×10^7 m^3.

The box model was initially employed to evaluate the hydrologic budget and Cl mass balance for the studied portion of the Indian River Lagoon. To examine the hydrologic budget we used previous estimates of terrestrial and marine SGD (Martin et al., 2007) and stream gauge data (U.S. Geological Survey) for the Eau Gallie River and Crane Creek. The total SGD to the studied portion of the Indian River Lagoon was computed by summing the previously determined estimates of terrestrial and marine SGD. The volume of seawater exchange between the lagoon and the coastal ocean was estimated by assuming that Cl is conservative and that the hydrologic budget is at steady-state. The salinity of the coastal ocean end-member was assumed to be 35‰, which is consistent with seawater off Florida's east coast (e.g., Smith, 1993; Swarzenski et al., 2006). The mass balance model was subsequently employed to investigate the cycling of the REEs within the studied portion of the Indian River Lagoon. A major objective was to evaluate whether geochemical reactions occurring in the subterranean estuary beneath the Indian River Lagoon influence the SGD flux of REEs to the overlying lagoon waters (e.g., see Duncan and Shaw, 2003). It is important to note, however, that the relatively simple box modeling approach used here only represents a first attempt to quantify REE fluxes in the Indian River Lagoon system. Additional sampling and data collection will no doubt help to constrain the model (e.g., see Roy et al., 2010).

4. RESULTS

4.1. Rare earth element concentrations

Rare earth element concentrations for waters from the Indian River Lagoon system waters are presented in Table 1, which also summarizes the shale-normalized Yb/Nd ratios for these waters, as well as presents mean REE concentrations for seawater taken from the literature. Concentrations of REEs in surface waters within the Indian River Lagoon (i.e., water column) decrease with increasing distance offshore. For example, at a distance of 5 m offshore, the Nd concentration of the lagoon water is 638 pmol kg^{-1}, whereas at a distance of 250 m from shore (i.e., water column station at CIRL-39) the Nd concentration is 164 pmol kg^{-1}. We note, however, that the general decrease in REE concentration with increasing distance from shore is punctuated by at least two local concentration maxima at 17.5 and 22.5 m offshore, where Nd concentrations are 389 and 354 pmol kg^{-1}, respectively (Table 1).

The same general decrease in REE concentration with increasing distance from shore is also observed for the terrestrial component of SGD, such that porewaters from multisampler EGN-0 exhibit higher REE concentrations

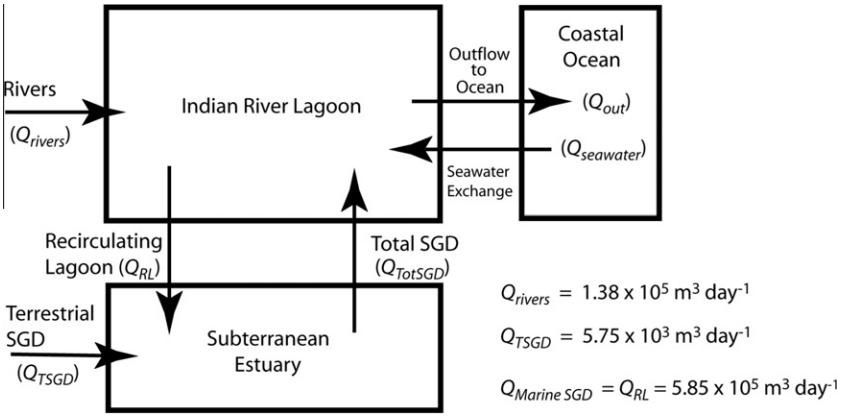

Fig. 3. Box model used to evaluate REE fluxes within the Indian River Lagoon system. The section of the Indian River Lagoon that corresponds to the mass balance model is shown in Fig. 1 and includes the portion of the Indian River Lagoon between the Eau Gallie River and Crane Creek. Marine SGD in the Indian River Lagoon system is largely lagoon water that circulates through the subterranean estuary, such that in the model $Q_{MarineSGD} = Q_{RL}$, where RL = recirculating lagoon water (see text for details). Thus the total SGD to the Indian River Lagoon consists of terrestrial SGD and recirculated lagoon water.

Table 1
Rare earth element concentrations (in pmol kg^{-1}) in waters from the Indian River Lagoon system, and average seawater computed with data from the literature. For the SGD samples, cmbsf = centimeters below sea floor.

	La	Ce	Pr	Nd	Sm	Eu	Gd	Tb	Dy	Ho	Er	Tm	Yb	Lu	$(Yb/Nd)_N$[a]
Water Column															
EGN-5, WC	559	1047	151	638	121	34.8	127	23.8	181	75.9	523	140	1388	317	29.9
EGN-10, WC	155	369	31.1	296	49.9	8.54	57.9	11	95.5	22.6	102	21.3	109	45.7	8.58
EGN-15, WC	300	574	74.5	362	71.4	21	91	17	114	30.5	131	28.3	239	52.7	9.06
EGN-17.5, WC	345	694	80.4	389	70.7	18.8	84.1	13	95.3	23.1	107	21.6	194	41.1	6.86
EGN-20, WC	157	294	33.2	191	33.1	13	50.1	7.48	62.9	15.1	65.2	21.6	101	20.8	7.29
EGN-22.5, WC	245	520	54.3	354	61.2	8.01	60	12	139	27.7	143	18.9	196	35.1	7.59
EGN-30, WC	141	228	16.6	127	20		36.8	6.59	48.5	13.2	48	9.48	71.7	11.7	7.76
CIRL-39, WC	143	256	24.2	164	27.2		44.9	7.96	51.4	7.6	38.1	7.13	42.2	8.31	3.53
Mean ± SD	256 ± 51.3	498 ± 97.9	58.2 ± 15.6	315 ± 58	56.8 ± 11.4	12.7 ± 4.28	69 ± 10.6	12.4 ± 2.03	98.4 ± 16.2	27 ± 7.5	145 ± 55.2	33.5 ± 15.3	293 ± 158	66.5 ± 36.1	
Terrestrial SGD															
EGN-0, 15 cmbsf	167	428	49.8	417	83	22.1	117	21.4	242	101	691	197	2216	533	72.8
EGN-0, 25 cmbsf	167	409	51.8	437	110	30.5	149	25.9	247	83.2	456	117	1087	222	34.1
EGN-0, 115 cmbsf	391	830	104	568	112	25.6	117	21.5	155	40.5	314	80.8	692	123	16.7
EGN-10, 25 cmbsf	121	275	24.7	231	29.1	5.87	37	5.45	64.5	11.3	50.1	8.44	95.4	17.9	5.66
EGN-10, 55 cmbsf	141	312	26.6	227	35	3.73	41.1	8.13	74.6	14.8	55.8	12.2	120	18.8	7.23
EGN-10, 115 cmbsf	137	307	27.5	217	28.1	3	30.2	5.36	47.9	9.06	42.7	9.71	84.4	14.5	5.32
Mean ± SD	187 ± 41.2	427 ± 84.5	47.4 ± 12.3	350 ± 59.6	66.3 ± 16.5	15.1 ± 5.02	82 ± 21.1	14.6 ± 3.8	139 ± 36.8	43.3 ± 16.2	268 ± 109	70.9 ± 31.2	716 ± 343	155 ± 82.9	
Total SGD															
EGN-10, 15 cmbsf	171	367	32.7	277	45.7	8.49	70.2	9.02	99.8	16.4	82.1	16.5	170	31.6	8.41
EGN-22.5, 6 cmbsf	141	289	27.5	258	50.5	5.6	45.9	8.69	73.2	14.4	64.7	10.2	93.4	12.3	4.96
EGN-22.5, 66 cmbsf	367	523	55.4	401	69.6	15.6	119	14.6	143	37.4	150	22.8	168	28.7	5.73
EGN-22.5, 106 cmbsf	677	1427	171	773	131	24.1	139	17.5	99.1	26.7	88.6	16.8	104	15.3	1.85
EGN-22.5, 146 cmbsf	617	1255	155	715	116	28.4	122	16.3	112	32	135	22.3	188	24.8	3.6
EGN-22.5, 186 cmbsf	1682	2879	362	2409	481	39.2	464	87	961	354	1703	361	2488	434	14.2
Mean ± SD[b]	395 ± 110	772 ± 237	88.4 ± 31	485 ± 109	82.6 ± 17.3	16.4 ± 4.37	99.3 ± 17.6	13.2 ± 1.84	105 ± 11.4	25.4 ± 4.42	104 ± 16.3	17.7 ± 2.2	145 ± 19.1	22.5 ± 3.76	
Rivers															
Eau Gallie river	320	742	117	627	180	82.5	268	39.7	250	59.7	201	35	291	60.3	6.35
Crane Creek	57.3	152	19.8	205	69.4	44.4	124	19.7	140	41.8	140	28.6	254	53.9	17
Mean ± SD[c]	123 ± 80.6	300 ± 180	41.1 ± 29.8	311 ± 129	97.1 ± 33.9	53.9 ± 11.7	160 ± 44.1	24.7 ± 6.12	168 ± 33.4	46.3 ± 5.48	155 ± 18.7	30.2 ± 1.96	263 ± 11.3	55.5 ± 1.96	
Seawater[d]	25.2 ± 1.92	7.35 ± 1.48	3.53 ± 0.38	17.9 ± 1.16	3.56 ± 0.23	0.91 ± 0.06	5.36 ± 0.3	0.74 ± 0.08	6.04 ± 0.35	1.5 ± 0.16	5.52 ± 0.31	0.76 ± 0.08	5.36 ± 0.36	0.91 ± 0.07	4.11

[a] PAAS normalized ratio.
[b] Does not include the EGN-22.5, 186 cmbsf sample (see text for discussion).
[c] Discharge-weighted mean and standard deviation.
[d] mean (±1 SD) of selected data from Piepgras and Jacobsen (1992), Westerlund and Öhman (1992), Bertram and Elderfield (1993), Sholkovitz et al. (1994), German et al. (1995), Nozaki and Zhang (1995), Zhang and Nozaki (1996), and Nozaki and Alibo (2003).

than those from EGN-10 (Table 1). More specifically, Nd concentrations range from 417 to 568 pmol kg^{-1} in porewaters collected from multisampler EGN-0 and from 217 to 277 pmol kg^{-1} in porewaters from EGN-10. However, the highest REE concentrations in porewaters from the Indian River Lagoon subterranean estuary occur at the freshwater–saltwater seepage face where terrestrial SGD mixes with marine SGD forming total SGD (Table 1). Here, porewater Nd concentrations reach values as high as 2409 pmol kg^{-1}.

Based on Cl^- concentrations and the position of the freshwater–saltwater seepage face (Tables 1 and 2; Fig. 2), porewaters from multisamplers EGN-0 and EGN-10 (i.e., 25, 55, and 115 cmbsf, where cmbsf = centimeters below sea floor) are employed in the mass balance model to represent the terrestrial SGD component, whereas porewaters from EGN-22.5, and the 15 cmbsf depth from EGN-10, reflect the total SGD (i.e., terrestrial SGD + marine SGD; Martin et al., 2007; Roy et al., 2010) in the model. Thus, Nd concentrations for terrestrial SGD range from 217 to 568 pmol kg^{-1}, exhibiting a mean (±SD) of 350 ± 59.6 pmol kg^{-1}, whereas for total SGD, Nd ranges from 258 to 2409 pmol kg^{-1}, with a mean (±SD) of 806 ± 333 pmol kg^{-1}. The deepest SGD sample from EGN-22.5 with the highest Nd concentration is assumed to be an outlier as its Nd value is more than a factor of 3 greater than the next highest Nd concentration (i.e., 773 pmol kg^{-1} for EGN-22.5, 106 cmbsf; Table 1). Thus, the mean (±SD) Nd concentration of total SGD (i.e., 485 ± 109 pmol kg^{-1}; Table 1) that we employ in our mass balance calculations excludes this presumed outlier.

Shale-normalized REE plots for porewaters and surface waters from the Indian River Lagoon system are all enriched in HREEs relative to LREEs (Fig. 4). Excluding the presumed outlier (EGN-22.5, 186 cmbsf), porewater and lagoon water nearest to shore (i.e., multisampler EGN-0, water column sample EGN-5, WC) exhibit the largest HREE enrichments (mean ± SD $(Yb/Nd)_{SN} = 38 \pm 12$; Table 1; Fig. 4). By comparison, shale-normalized Yb/Nd ratios for seawater are typically around 4 (Table 1). The shale-normalized REE patterns further demonstrate that porewater within the Indian River Lagoon subterranean estuary consists of both the terrestrial component of SGD (e.g., Fig. 4b and c), as well as recirculated Indian River Lagoon water (Fig. 4a).

4.2. REE solution complexation

The results of the solution complexation modeling for the REEs in waters of the Indian River Lagoon system are shown in Fig. 5. The average major solute compositions of terrestrial SGD, total SGD, and the lagoon water column (Table 2) were used in the model calculations. The model predicts that the REEs chiefly occur in solution within Indian River Lagoon waters complexed with carbonate ions (Fig. 5). For example, the percentage of each REE complexed with carbonate ions (i.e., $LnCO_3^+ + Ln(CO_3)_2^-$, where Ln represents the individual REE) ranges from 76% for La to 98% for Lu in terrestrial SGD, from 58% for La to 97% for Lu in total SGD, and from 89% for La to 99% for Lu in the lagoon water column. Carbonato complexes ($LnCO_3^+$) predominate in the neutral pH, terrestrial SGD accounting for 60–80% of each REE in solution, whereas in the higher pH water column samples, the dicarbonato complex ($Ln(CO_3)_2^-$) is the principal dissolved form for all REEs except La (Fig. 5). The model predicts that REE carbonato complexes also predominate in the total SGD, except for Yb and Lu, which occur chiefly as dicarbonato complexes (Fig. 5).

4.3. Hydrologic and chloride mass balance model

United States Geological Survey stream gauge data for the Eau Gallie River (USGS 02249007) between January 1991 and September 2004 (average 3.46×10^4 m^3 day^{-1}, $n = 4555$) and Crane Creek (USGS 02249518) between January 1987 and September 2004 (average 1.04×10^5 m^3 day^{-1}, $n = 6377$) provides an estimate of the mean discharge of the two rivers ($Q_{rivers} = 1.39 \times 10^5$ m^3 day^{-1}; Table 3) into the studied portion of the Indian River Lagoon. For the terrestrial and marine components of SGD to the Indian River Lagoon, the estimates of Martin et al. (2007) of 1.15 and 117 m^3 day^{-1} per meter of shoreline, respectively, are employed. The terrestrial and marine SGD fluxes (i.e., Q_{TSGD}, $Q_{MarineSGD}$) are recalculated for the entire 5 km seepage front between the Eau Gallie River and Crane Creek giving 5.75×10^3 and 5.85×10^5 m^3 day^{-1}, respectively (Table 3). Hence, total SGD to the Indian River Lagoon (i.e., $Q_{TotSGD} = Q_{TSGD} + Q_{MarineSGD}$) exceeds river discharge by a factor of four. Assuming that Cl is conservative, the Cl mass balance for the Indian River Lagoon subterranean estuary can be written as:

$$[Cl^-]_{TSGD}Q_{TSGD} + [Cl^-]_{lagoon}Q_{MarineSGD} = [Cl^-]_{TotSGD}Q_{TotSGD} \quad (1)$$

where $[Cl^-]_{TSGD}$, and $[Cl^-]_{lagoon}$ are the mean Cl concentrations of terrestrial SGD and the Indian River Lagoon water column, respectively (Table 3; Fig. 3). The Cl concentration of total SGD, $[Cl^-]_{TotSGD}$, computed by solving Eq. (1) (i.e., 335 mmol kg^{-1}) is identical to the mean (±SD) of the Cl concentrations measured in the lagoon water column (338 ± 15 mmol kg^{-1}; Table 3), as well as measured in porewater samples from multisamplers EGN-30 and CIRL-39 (335 ± 8.55 mmol kg^{-1}; data not shown). These observations further support that recirculating lagoon water is the principal source of SGD within the Indian River Lagoon subterranean estuary.

Eq. (1) can be recast into terms of the Cl fluxes as:

$$J^{Cl}_{TSGD} + J^{Cl}_{MarineSGD} = J^{Cl}_{TotSGD} \quad (2)$$

where, for example, $J^{Cl}_{TSGD} = [Cl^-]_{TSGD}Q_{TSGD}$. The respective Cl fluxes are listed in Table 3 for terrestrial SGD, total SGD, and marine SGD (i.e., recirculated lagoon water). The computed Cl fluxes also indicate that the terrestrial component of SGD has a negligible impact on the salt budget in the subterranean estuary beneath the Indian River Lagoon because J^{Cl}_{TSGD} is almost four orders of magnitude smaller than $J^{Cl}_{MarineSGD}$. Hence, the amount of Cl entering the bottom sediments of the Indian River Lagoon as marine SGD (i.e., recirculating lagoon water; 198(±8.78) × 10^6 mol day^{-1}) is essentially equal to that leaving the subterranean estuary as total SGD (198(±8.8) × 10^6 mol day^{-1}).

Table 2
Geochemical composition of waters from the Indian River Lagoon system. Major solute compositions are in mmol kg^{-1}, and dissolved oxygen (DO), Fe, and sulfide concentrations are in μmol kg^{-1}. Ionic strength is reported in mol kg^{-1}.

	pH	Temp. (°C)	DO (μmol kg^{-1})	Ca (mmol kg^{-1})	Mg (mmol kg^{-1})	Na (mmol kg^{-1})	K (mmol kg^{-1})	Cl (mmol kg^{-1})	SO_4 (mmol kg^{-1})	Alk (mmol kg^{-1})	Fe (μmol kg^{-1})	S(-II) (μmol kg^{-1})	Ionic strength (mol kg^{-1})	SI[b] (goethite)
Water column														
EGN-5, WC	8.63	28.9	337	6.47		204	4.46	240	12.1	2.44	0.375	8	0.2677	
EGN-10, WC	8.58	28.8	398	5.18		295	6.45	341	17.3	2.43		8	0.3769	
EGN-15, WC	8.42	26.2	440	14.4	55.4	473	10.5	349	17.8	2.64	0.176	5	0.612	
EGN-17.5, WC	8.57	20.6	351			307	6.39	343	18.3	3.17		3	0.3776	
EGN-20, WC	8.13	21.9	275			325	6.86	364	19.5	2.68		9	0.4005	
EGN-22.5, WC	8.31	21.9	312			315	6.63	329	17.6	2.71	0.056	2.87	0.3721	
EGN-30, WC	8.34	26.9	281			320	6.7	357	19.2	2.48	0.054	11	0.3935	
CIRL-39, WC	8.26	24	236			332	7	384	19.8	2.35			0.4159	
Mean ± SD[a]	8.41 ± 0.06	23.6 ± 1.6	329 ± 23.8	8.68 ± 2.88		321 ± 26	6.87 ± 0.58	338 ± 15	17.7 ± 0.86	2.61 ± 0.09	0.165 ± 0.076	6.7 ± 1.2	0.402 ± 0.034	
Terrestrial SGD														
EGN-0, 15 cmbsf	6.78	24.7	22.5	1.07	0.31	0.75	0.05	2	0.2	1.75	0.027	7	0.005	−0.478
EGN-0, 25 cmbsf	6.76	24.5	32.8	0.84		0.75	0.04	2	0.2	1.51		6	0.0039	
EGN-0, 115 cmbsf	7.19	25.8	34.4	1.42	0.37	1.08	0.05	2	0.3	2.91	0.108	8	0.0067	−0.48
EGN-10, 25 cmbsf	7.34	26.6	48.4	3.13		54.9	0.93	13	1.1	3.73	2.18	8	0.0434	−0.482
EGN-10, 55 cmbsf	7.31	26.6	26.6	1.96	1.08	3.93	0.07	5	0.6	3.61	0.835	12	0.0127	−0.481
EGN-10, 115 cmbsf	7.38	26.6	26.3	1.92	1.04	3.47	0.06	4	0.6	3.89	9.236	5	0.012	−0.481
Mean ± SD[a]	7.13 ± 0.12	25.8 ± 0.4	31.8 ± 3.78	1.72 ± 0.34	0.7 ± 0.21	10.8 ± 8.83	0.2 ± 0.15	4.67 ± 1.74	0.5 ± 0.14	2.9 ± 0.43	2.42 ± 1.73	7.51 ± 0.99	0.014 ± 0.006	−0.481 ± 0.001
Total SGD														
EGN-10, 15 cmbsf	7.13	26.4	95.6	6.4		115	2.3	132	6.8	3.1	1.96	200	0.1539	−0.482
EGN-22.5, 6 cmbsf	7.43	26.2	25			313	6.32	347	18.3	4.53	1.57	422	0.3826	−0.483
EGN-22.5, 66 cmbsf	7.23	22.7	41.6	11.4		226	4.09	270	13.5		13.4	156	0.3064	−0.477
EGN-22.5, 106 cmbsf	7.11	22.8	29.1	14.3		157	1.76	190	8.7	3.52	286	8.6	0.2257	−0.476
EGN-22.5, 146 cmbsf	7.09	23.4	28.1	10.7		188	2.81	221	11.1	3.8	261		0.2551	−0.477
EGN-22.5, 186 cmbsf	7.15	26.5	14.1	10.5		203	3.4	234	11.9	4.38	196	25.1	0.274	−0.483
Mean ± SD[a]	7.19 ± 0.05	24.2 ± 0.69	38.9 ± 11.9	10.6 ± 1.26		200 ± 27.4	3.45 ± 0.66	335 ± 14.9[c]	11.7 ± 1.64	3.87 ± 0.27	127 ± 55.5	162 ± 74.6	0.266 ± 0.031	−0.48 ± 0.001
Rivers														
Eau Gallie River	7.73	23.1						9.97						
Crane Creek	7.62	22.4						10.7						

[a] Mean values were used in the REE solution complexation model.
[b] SI = saturation index (log IAP/K_{sp}) computed with the React program of the Geochemist's Workbench® (version 7; Bethke, 2008).
[c] Calculated using Eq. (1).

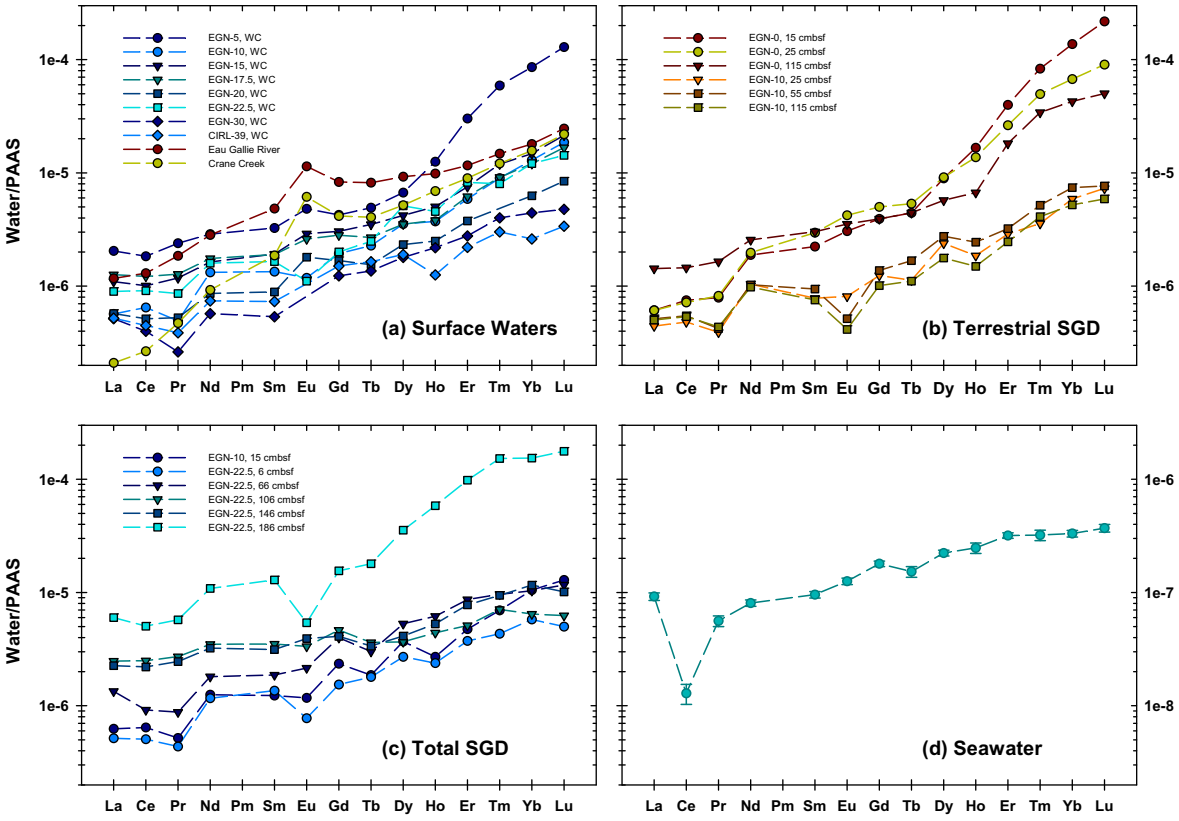

Fig. 4. Shale-normalized REE plots of waters from the Indian River Lagoon system showing: (a) Indian River Lagoon water column, Eau Gallie River, and Crane Creek samples; (b) terrestrial component of SGD beneath the Indian River Lagoon; (c) the total SGD (terrestrial SGD + recirculated marine SGD) at the freshwater–saltwater seepage face; and (d) the mean seawater data (±1 SD) presented in Table 1. Note, the scale of the ordinate for the mean seawater sample differs from the Indian River Lagoon water samples by a factor of 100 lower. Rare earth elements concentrations for all water samples are normalized to the Post Archean Australian Shale (PAAS) composite (Nance and Taylor, 1976). See on-line version for colors.

Because the discharge weighted mean Cl concentration for the two rivers entering the studied portion of the Indian River Lagoon is more than 30 times lower than the average Cl concentration of the lagoon water (Table 3), most of the Cl within the Indian River Lagoon comes from exchange with coastal seawater. Seawater exchange between the coastal ocean and the Indian River Lagoon is estimated using Cl and water mass balances for the Indian River Lagoon (Fig. 3). Chloride mass balance for the lagoon is expressed as:

$$[Cl^-]_{rivers}Q_{rivers} + [Cl^-]_{TotSGD}Q_{TotSGD} + [Cl^-]_{seawater}Q_{seawater} = [Cl]_{lagoon}Q_{MarineSGD} + [Cl^-]_{lagoon}Q_{out} \quad (3)$$

where $[Cl^-]_{seawater}$ is the Cl concentration of seawater (Table 1; Fig. 3), and $Q_{seawater}$ is the volumetric exchange of seawater with the studied portion of the Indian River Lagoon. Water mass balance in the Indian River Lagoon implies,

$$Q_{rivers} + Q_{seawater} + Q_{TotSGD} = Q_{out} + Q_{MarineSGD}, \quad (4)$$

whereas water mass balance in the subterranean estuary can be written as:

$$Q_{TSGD} + Q_{MarineSGD} = Q_{TotSGD}. \quad (5)$$

Combining Eqs. (4) and (5) yields:

$$Q_{out} = Q_{rivers} + Q_{seawater} + Q_{TSGD}. \quad (6)$$

Substituting Eq. (6) into Eq. (3), and solving for $Q_{seawater}$ gives:

$$Q_{seawater} = \frac{[Cl^-]_{lagoon}(Q_{RL} + Q_{rivers} + Q_{TSGD}) - [Cl^-]_{rivers}Q_{rivers} - [Cl^-]_{TotSGD}Q_{TotSGD}}{[Cl^-]_{seawater} - [Cl^-]_{lagoon}}. \quad (7)$$

Using the values in Table 3 for mean chloride concentrations and the corresponding volumetric discharges, Q_i, we estimate that seawater exchange with the studied portion of the Indian River Lagoon is on the order of $2.24(\pm 0.69) \times 10^5$ m^3 day^{-1} (Fig. 3; Table 3). To evaluate whether this amount of seawater exchange is reasonable, we calculate the residence time of water and Cl in the studied portion of the Indian River Lagoon using our estimated volumetric discharges and Cl fluxes. For water, we obtain a

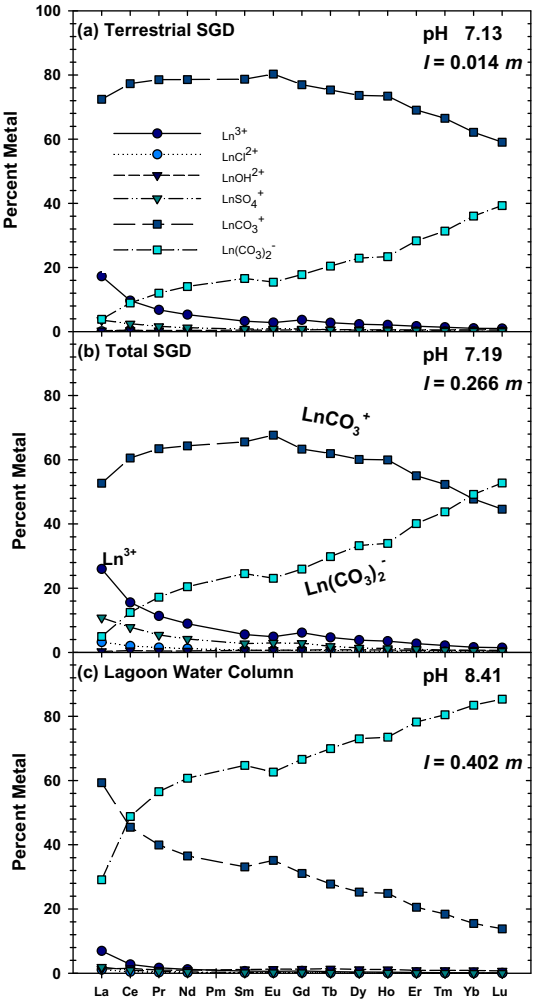

Fig. 5. Results of the solution complexation model for (a) terrestrial SGD, (b) total SGD, and (c) Indian River Lagoon water column samples, where Ln represents each individual REE. Mean major solute and water quality parameters for each end-member water that were used in the model calculations are listed in Table 2. Plots show the relative percent of each REE that occurs in solution as any given aqueous complex. See on-line version for colors.

residence time of 14.2 ± 1 days, whereas the estimated residence time for Cl is 14.2 ± 1.1 days. These residence times are identical, and similar to the 18 days flushing time for this portion of the Indian River Lagoon computed with a 1-D numerical model (Smith, 1993), which lends credibility to the applicability of the mass balance model presented here for the Indian River Lagoon system.

4.4. REE mass balance

Using the calculated, mean Nd concentrations measured in terrestrial SGD, total SGD, the Eau Gallie River and Crane Creek, and the lagoon water column as an example for the other REEs (Table 1), along with the volumetric water fluxes (Table 3), we calculate Nd fluxes for the studied portion of the Indian River Lagoon system (Table 4). It is important to note, however, that because our REE data are for a single point in time, concentrations and REE fluxes may vary seasonably. For example, residence times of fresh groundwater in the Surficial Aquifer range between 5 and 7 months, indicating that wet season subtropical precipitation is reflected in SGD a half year later (Smith et al., 2008a). Nonetheless, long-term head-level monitoring and SGD measurements demonstrate that in the absence of tropical cyclones during the wet season, terrestrial SGD from the Surficial Aquifers varies by less than a factor of 4 between the wet and dry seasons (Smith et al., 2008b). The mean Nd concentration for the seawater component is computed using values published in the literature (Table 1; Fig. 4).

Balancing Nd fluxes for the lagoon first, we have $J^{Nd}_{in} = J^{Nd}_{out}$, which upon expansion gives the following expression:

$$J^{Nd}_{rivers\text{-}eff} + J^{Nd}_{seawater} + J^{Nd}_{TotSGD} = J^{Nd}_{MarineSGD} + [Nd]_{lagoon} Q_{out} \quad (8)$$

where $J^{Nd}_{rivers\text{-}eff} = Q_{rivers}[Nd]_{rivers\text{-}eff}$ is the effective river flux of Nd into the Indian River Lagoon following 70% removal of Nd (i.e., $[Nd]_{rivers\text{-}eff}$) in the estuarine portions of the Eau Gallie River and Crane Creek, and $[Nd]_{lagoon}$ is the mean Nd concentration of the lagoon waters (Table 4). The effective river flux accounts for REE removal by salt-induced,

Table 3
Mean chloride concentrations (± 1 SD of the mean) and fluxes used in the mass balance model.

	Cl (mmol kg^{-1})	Q[a] (m^3 day^{-1})	J_{Cl} (mol day^{-1})
Terrestrial SGD	4.67 ± 1.74	5.75×10^3	$26.9(\pm 10) \times 10^3$
Marine SGD	338 ± 15[b]	5.85×10^5	$198(\pm 8.78) \times 10^6$
Total SGD	335 ± 14.9[c]	5.91×10^5	$198(\pm 8.8) \times 10^6$
Rivers	10.5 ± 0.23[d]	1.38×10^5	$1.45(\pm 0.03) \times 10^6$
Lagoon	338 ± 15		
Seawater	545.88[e]	$2.24(\pm 0.69) \times 10^5$	$122(\pm 37.7) \times 10^6$

[a] Measured variability of SGD fluxes is estimated to be ±50%. The total SGD discharging from the subterranean estuary is $Q_{TotSGD} = Q_{TSGD} + Q_{MarineSGD}$, which is equivalent to $Q_{TSGD} + Q_{RL}$, where RL is recirculated Indian River Lagoon water (see Martin et al., 2007 and Fig. 3).
[b] Mean ± SD Cl concentration of IRL water column samples (see Table 1).
[c] Calculated using Eq (1).
[d] Discharge weighted mean ± SD for the Eau Gallie River and Crane Creek (see Martin et al., 2007).
[e] Assumes a salinity of 35‰ for the coastal ocean (see text for details).

Table 4
Mean Nd concentrations (± 1 SD of the mean), mean discharge of groundwater and surface waters, and neodymium fluxes for the studied portion of the Indian River Lagoon.

	Nd (pmol kg^{-1})	Q (m^3 day^{-1})	J_i^{Nd} (mol day^{-1})
Terrestrial SGD	350 ± 59.6	5.75×10^3	$2.01(\pm 0.34) \times 10^{-3}$
Marine SGD	315 ± 58	5.85×10^5	$184(\pm 33.9) \times 10^{-3}$
Total SGD	485 ± 109	5.91×10^5	$287(\pm 64.4) \times 10^{-3}$
Rivers	311 ± 129[a]	1.38×10^5	$[12.7(\pm 5.27) \times 10^{-3}]$[b]
Lagoon	315 ± 58		
Seawater	17.9 ± 1.16	$2.24(\pm 0.69) \times 10^5$	$4.01(\pm 1.26) \times 10^{-3}$
	J_{in}^{Nd} (mol day^{-1})	J_{out}^{Nd} (mol day^{-1})	J_{net}^{Nd} (mol day^{-1})
Lagoon	$304(\pm 64.7) \times 10^{-3}$[c]	$300(\pm 88.8) \times 10^{-3}$[d]	
Sediments	$186(\pm 33.9) \times 10^{-3}$[e]	$287(\pm 64.4) \times 10^{-3}$	$100(\pm 72.8) \times 10^{-3}$[f]

[a] Discharge weighted mean Nd concentration of Eau Gallie River and Crane Creek.
[b] Effective river flux that assumes that 70% of the river borne Nd is removed in these estuaries.
[c] $J_{rivers\text{-}eff}^{Nd} + J_{seawater}^{Nd} + J_{TotSGD}^{Nd}$.
[d] $J_{MarineSGD}^{Nd} + [Nd]_{lagoon}(Q_{rivers} + Q_{TSGD} + Q_{seawater})$.
[e] $J_{MarineSGDs}^{Nd} + J_{TSGD}^{Nd}$.
[f] $J_{TotSGD}^{Nd} - (J_{Marine}^{Nd} + J_{TSGD}^{Nd})$.

colloid coagulation as fresh river water mixes with brackish estuarine waters, which, on average, removes ~70% of the dissolved river-borne Nd load (Goldstein and Jacobsen, 1987; Sholkovitz, 1993, 1995; Sholkovitz and Szymczak, 2000; Lawrence and Kamber, 2006). Removal of REEs in the subterranean estuary by this process is, however, not significant as the marine component of SGD is already saline (Duncan and Shaw, 2003). Neodymium inputs to the Indian River Lagoon from the effective river flux, seawater exchange, and total SGD sum to 304 ± 64.7 mmol day^{-1}, whereas the Nd flux out of the lagoon via input to the subterranean estuary by marine SGD (i.e., recirculating lagoon water) and export to the coastal ocean is estimated to be 300 ± 88.8 mmol day^{-1} (Fig. 3; Table 4). These values indicate that the Nd concentrations within the Indian River Lagoon water column are roughly at steady-state with respect to the Nd fluxes into and out of the lagoon. We estimate a residence time for Nd of 14.1 ± 3.2 days for the studied portion of the lagoon, which is identical to the estimated water and Cl residence times, and close to the flushing time estimated by Smith (1993).

The mass balance for Nd in the subterranean estuary beneath the Indian River Lagoon can be represented by:

$$J_{TSGD}^{Nd} + J_{MarineSGD}^{Nd} = J_{TotSGD}^{Nd}. \quad (9)$$

Using the mean Nd concentrations for terrestrial SGD and for the Indian River Lagoon water column, along with the corresponding volumetric water fluxes, Q_{TSGD} and $Q_{MarineSGD}$, respectively, the flux into the subterranean estuary, J_{in}^{Nd}, can be calculated as $J_{TSGD}^{Nd} + J_{MarineSGD}^{Nd}$, which yields a value of 186 ± 33.9 mmol Nd day^{-1} (Table 4). The flux of Nd out of the subterranean estuary and into the overlying coastal waters of the Indian River Lagoon is equal to $J_{TotSGD}^{Nd} = Q_{TotSGD}[Nd]_{TotSGD}$. Computing this flux using the mean Nd concentration of total SGD and the associated total SGD flux of water, Q_{TotSGD}, yields a value of 287 ± 64.4 mmol Nd day^{-1}, which is 100 mmol Nd day^{-1} larger than the model computed influx to the subterranean estuary (Table 4). Consequently, the subterranean estuary is not at steady-state with respect to the Nd fluxes, and instead represents a net flux of Nd to the overlying coastal waters of the Indian River Lagoon. We note that owing to the variability in the measured terrestrial and marine SGD fluxes (Table 3), the net SGD Nd flux to the overlying coastal waters could be as low as 10 mmol Nd day^{-1} or as large as 338 mmol Nd day^{-1}.

The same mass balance approach can be applied to the entire REE series. Calculated fluxes into and out of the Indian River Lagoon subterranean estuary are presented in Table 5. As with Nd, fluxes of REEs into the subterranean estuary, J_{in}^{REE}, include terrestrial SGD and marine SGD (i.e., recirculated lagoon water), whereas the REEs are exported from the subterranean estuary to the overlying lagoon water, J_{out}^{REE}, via total SGD (Fig. 3). The difference between J_{out}^{REE} and J_{in}^{REE} again represents the net flux of each REE from the subterranean estuary to the overlying coastal waters. The computed net fluxes reveal that more of each LREE and MREE is exported from the subterranean estuary to the overlying coastal waters of the Indian River Lagoon than imported into the subterranean estuary via terrestrial SGD and recirculating lagoon waters (Table 5). However, the opposite is observed for REEs heavier than Ho such that the amount of each of these HREEs imported into the subterranean estuary exceeds that which is exported to the coastal lagoon waters via total SGD. Therefore, the subterranean estuary beneath the Indian River Lagoon appears to act as a net source of LREEs and MREEs to the overlying coastal waters and as a sink for the HREEs.

5. DISCUSSION

5.1. SGD fluxes of REEs in the Indian River Lagoon subterranean estuary

Our current best estimate of the total SGD Nd flux to the studied portion of the Indian River Lagoon is 287 ± 64.4 mmol day^{-1}, which is ~150-fold larger than

Table 5
Fluxes of REEs in mmol day^{-1} for the Indian River Lagoon subterranean estuary.

	J^{REE}_{TSGD}	$J^{REE}_{MarineSGD}$	J^{REE}_{TotSGD}	J^{REE}_{in} [a]	J^{REE}_{out} [b]	J^{REE}_{net} [c]
La	1.08 ± 0.24	150 ± 30	233 ± 65	151 ± 30	233 ± 65	82.6 ± 71.6
Ce	2.46 ± 0.49	291 ± 57.3	456 ± 140	294 ± 57.3	456 ± 140	162 ± 151
Pr	0.27 ± 0.07	34 ± 9.13	52.2 ± 18.3	34.3 ± 9.13	52.2 ± 18.3	17.9 ± 20.5
Nd	2.01 ± 0.34	184 ± 33.9	287 ± 64.4	186 ± 33.9	287 ± 64.4	100 ± 72.8
Sm	0.38 ± 0.09	33.2 ± 6.67	48.8 ± 10.2	33.6 ± 6.67	48.8 ± 10.2	15.2 ± 12.2
Eu	0.09 ± 0.03	7.43 ± 2.5	9.69 ± 2.58	7.52 ± 2.5	9.69 ± 2.58	2.18 ± 3.6
Gd	0.47 ± 0.12	40.4 ± 6.2	58.7 ± 10.4	40.8 ± 6.2	58.7 ± 10.4	17.8 ± 12.1
Tb	0.08 ± 0.02	7.25 ± 1.19	7.8 ± 1.09	7.34 ± 1.19	7.8 ± 1.09	0.46 ± 1.61
Dy	0.80 ± 0.21	57.6 ± 9.48	62.1 ± 6.74	58.4 ± 9.48	62.1 ± 6.74	3.69 ± 11.6
Ho	0.25 ± 0.09	15.8 ± 4.39	15 ± 2.61	16 ± 4.39	15 ± 2.61	−1.03 ± 5.11
Er	1.54 ± 0.63	84.8 ± 32.3	61.5 ± 9.63	86.4 ± 32.3	61.5 ± 9.63	−24.9 ± 33.7
Tm	0.41 ± 0.18	19.6 ± 8.95	10.5 ± 1.3	20 ± 8.95	10.5 ± 1.3	−9.54 ± 9.05
Yb	4.12 ± 1.97	171 ± 92.4	85.7 ± 11.3	176 ± 92.5	85.7 ± 11.3	−89.8 ± 93.1
Lu	0.89 ± 0.48	38.9 ± 21.1	13.3 ± 2.22	39.8 ± 21.1	13.3 ± 2.22	−26.5 ± 21.2

[a] $J^{REE}_{in} = J^{REE}_{TSGD} + J^{REE}_{MarineSGD}$.
[b] $J^{REE}_{out} = J^{REE}_{TotSGD}$.
[c] $J^{REE}_{net} = J^{REE}_{TotSGD} - (J^{REE}_{TSGD} + J^{REE}_{MarineSGD})$.

our best estimate of the terrestrial SGD Nd flux of 2.01 ± 0.34 mmol day^{-1} (Table 4). Because this estimate does not include the possible outlier discussed above, the total SGD Nd flux may be even larger. The net SGD Nd flux, which represents the amount of Nd that is exported from the sediments of the subterranean estuary to the overlying coastal waters via SGD, is estimated to be on the order of ~100 mmol Nd day^{-1} (Table 4), or nearly seven times larger than the effective river Nd flux. Therefore, in the case of the Indian River Lagoon system, the effect of SGD is to add Nd to these coastal waters.

The results of these calculations are schematically shown in Fig. 6, which presents the mean, discharge-weighted, shale-normalized REE pattern of the flux into the Indian River Lagoon subterranean estuary (i.e., terrestrial SGD + recirculating lagoon water) along with the mean, shale-normalized REE pattern of the outflow from the subterranean estuary (i.e., total SGD). Fig. 6 demonstrates that the mean, shale-normalized REE signature of water entering the Indian River Lagoon subterranean estuary is more enriched in HREEs compared to LREEs than the flux of water leaving the subterranean estuary as total SGD. These observations can be further quantified by comparison of the shale-normalized Yb/Nd ratio (i.e., $(Yb/Nd)_{SN}$), which is 12.9 for the inflow water (terrestrial SGD + recirculated marine SGD) and 4.1 for the outflow water (total SGD). We note that the $(Yb/Nd)_{SN}$ ratio of total SGD is similar to that of seawater (i.e., ~4; Table 1; Fig. 4). The difference between the shale-normalized REE patterns of the inflow and outflow illustrates the changes in REE concentrations and fractionation patterns that occur as groundwater flows into and through the subterranean estuary beneath the Indian River Lagoon. Specifically, geochemical reactions affecting REEs within the Indian River Lagoon subterranean estuary lead to a general flattening of shale-normalized REE patterns as LREEs and MREEs are added to groundwater flowing through these sediments and HREEs are retained in the sediments. These observations are remarkable as geochemical reactions that fractionate REEs in surface estuaries (i.e., removal in low-salinity regions by salt-induced, colloid coagulation; mobilization in mid- to high-salinity regions) tend to further enrich HREEs in solution relative to LREEs and MREEs compared to shale (e.g., Elderfield et al., 1990; Sholkovitz, 1992, 1993, 1995; Sholkovitz and Szymczak, 2000; Lawrence and Kamber, 2006).

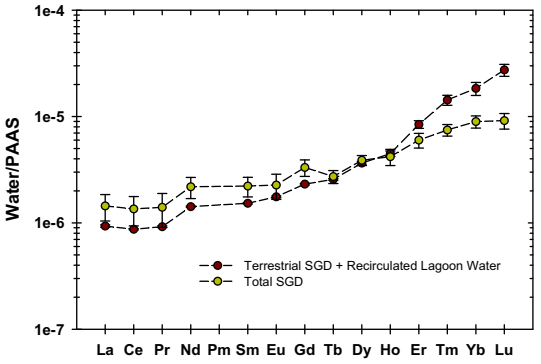

Fig. 6. Comparison of the shale-normalized REE patterns of water entering and exiting the Indian River Lagoon subterranean estuary. The shale-normalized REE pattern for water entering the subterranean estuary beneath the Indian River Lagoon is represented by the discharge-weighted mean (± SD) REE concentrations for the terrestrial SGD and recirculated lagoon water, whereas the mean shale-normalized pattern of the total SGD samples represent the REE pattern of SGD exiting the subterranean estuary. See on-line version for colors.

5.2. REE cycling in the Indian River Lagoon subterranean estuary

Rare earth element concentrations in porewaters from the Indian River Lagoon subterranean estuary are more than 10–100 times greater than typical open-ocean seawater REE concentrations (e.g., Table 1). The highest REE concentrations occur in SGD from the vicinity of the freshwater–saltwater seepage face (i.e., EGN-22.5; Figs. 2 and 4).

These REE concentrations are too high to originate from binary mixing of seawater with terrestrial SGD, and instead point to geochemical reactions occurring within the subterranean estuary as an important source of REEs to SGD, and hence, the overlying lagoon waters. This interpretation is consistent with the observations of Duncan and Shaw (2003) who argued that geochemical reactions occurring in a subterranean estuary along the coast of South Carolina, USA, appear to add REEs to local coastal waters.

A number of geochemical reactions could play important roles in mobilizing REEs within the Indian River Lagoon subterranean estuary. For example, mobilization of REEs may in part reflect the increase in salinity across the seepage face within the subterranean estuary. It is well documented that REEs are released from sediments in the mid- to high-salinity regions of surface estuaries (Sholkovitz, 1993, 1995; Sholkovitz and Szymczak, 2000). Furthermore, Tang and Johannesson (2010) demonstrated in laboratory experiments that an increase in ionic strength from 0.01 to 0.1 mol kg^{-1} dramatically suppresses REE adsorption onto Fe(III) oxide/oxyhydroxide-coated quartz sands. These results imply that mixing of recirculating marine SGD with terrestrial SGD in subterranean estuaries could induce REE desorption from aquifer mineral surface sites, thereby contributing to the REE flux to coastal waters (Tang and Johannesson, 2010). However, REE concentrations are, at best, only weakly associated with ionic strength in SGD from the Indian River Lagoon subterranean estuary ($r = 0.35$, Nd; $r = 0.31$, Gd; $r = -0.12$, Yb), and none of these relationships are statistically significant. Hence, although salinity-related REE release to SGD in the Indian River Lagoon subterranean estuary likely contributes to the overall net flux of LREEs and MREEs exported to the overlying coastal lagoon waters, it does not appear to be the predominant geochemical reaction mobilizing REEs in this subterranean estuary. Alternatively, because Fe diagenesis in the Indian River Lagoon subterranean estuary also chiefly occurs at the freshwater–saltwater seepage face similar to the REEs (Roy et al., 2010), geochemical reactions controlling the Fe cycle in the subterranean estuary represent another possible mechanism for REE mobilization.

The Fe cycle in the Indian River Lagoon subterranean estuary has recently been discussed in detail (Roy et al., 2010). As mentioned above Fe(III) oxide/oxyhydroxide coatings on the subterranean estuary sediments are ubiquitous, clearly indicating precipitation of Fe(III) oxides/oxyhydroxides under sub-aerial conditions when sea-level was lower and the subterranean estuary was further offshore (e.g., during the Last Glacial Maximum; Hartl, 2006; Roy et al., 2010). With rising sea-level, the freshwater–saltwater seepage face has moved landward, flooding these orange, terrestrial sediments and consequently impacting the Fe cycle such that it now involves three distinct steps (Roy et al., 2010). First, reductive dissolution of Fe(III) oxides/oxyhydroxides occurs within these orange sediments of the subterranean estuary when hypoxic terrestrial SGD mixes with recirculating marine SGD. Reduction of Fe(III) is likely driven by the introduction of labile dissolved organic carbon (DOC) entrained within the DOC-rich marine SGD (e.g., Cherrier et al., 2007; Roy et al., 2010). Second, the resulting dissolved Fe(II) is transported upwards with advecting groundwater into the sulfate reduction zone at the base of the overlying black, marine sediments, where it is subsequently precipitated as Fe-sulfides (Roy et al., 2010). Third, some of these Fe-sulfides are redissolved near the sediment–water interface where bioirrigation provides dissolved oxygen from the overlying, oxic lagoon waters (Roy et al., 2010).

Iron cycling within the Indian River Lagoon subterranean estuary differs from that of Waquoit Bay on Cape Cod, Massachusetts, where Fe oxidation and subsequent precipitation of Fe(III) oxides/oxyhydroxides predominates (Charette and Sholkovitz, 2002; Testa et al., 2002; Charette et al., 2005; Spiteri et al., 2006, 2008). At Waquoit Bay, the large tidal range (~1.5 m) regularly exposes the subterranean estuary to the atmosphere. Consequently, dissolved Fe(II) in hypoxic, terrestrial SGD oxidizes and precipitates within the subterranean estuary as terrestrial SGD mixes with oxic marine SGD (Charette and Sholkovitz, 2002). Because the Indian River Lagoon is microtidal, the corresponding subterranean estuary is not regularly exposed to the atmosphere, and hence, remains submerged and anoxic (Roy et al., 2010). Furthermore, Fe(III) oxides/oxyhydroxide precipitation in the subterranean estuary beneath Waquoit Bay is also apparently driven by an increase in pH from 5.5 nearshore, to ~8 at the freshwater–saltwater seepage face (Spiteri et al., 2006). In contrast, pH changes little within the Indian River Lagoon subterranean estuary and thus does not affect dissolved Fe concentrations in the same manner as in the Waquoit Bay subterranean estuary (Table 2; Roy et al., 2010). Therefore, Fe cycling in subterranean estuaries can be dominated by oxidation (Waquoit Bay, Massachusetts, USA; Patos Lagoon, Brazil) or reduction (Indian River Lagoon, Florida; North Inlet, South Carolina; Moses Hammock, Georgia, USA), which depends of the composition of the sediments and porewaters, as well as the "structure" (e.g., large tidal range vs. microtidal) of the subterranean estuary (Charette and Sholkovitz, 2002; Duncan and Shaw, 2003; Snyder et al., 2004; Windom et al., 2006; Roy et al., 2010).

The high dissolved Fe and low dissolved oxygen concentrations for the SGD samples presented in Table 2 further supports the Fe cycling model of Roy et al. (2010). That Fe(III) reduction predominates in the studied portion of the subterranean estuary is also supported by the low NO_3^- concentrations (<0.3 μmol kg^{-1}) measured in SGD seaward of the EGN-0 multisampler (Cherrier et al., 2007). Furthermore, all of the SGD from the Indian River Lagoon sampled in this study are undersaturated with respect to goethite (Table 2), indicating that reductive dissolution of goethite is thermodynamically favorable. Taken together, these data point to Fe(III) reduction as the chief redox buffering reaction controlling the redox conditions within the portion of the subterranean estuary sampled.

Similar to the REEs, dissolved Fe concentrations at the freshwater–saltwater seepage face are also substantially higher than can be explained by simple mixing of seawater and terrestrial SGD, indicating *in situ* reactions are responsible for the elevated Fe concentrations (Roy et al., 2010). Because REEs strongly adsorb onto Fe(III) oxides/oxyhy-

droxides in marine environments (Quinn et al., 2004, 2006a,b), diagenetic reactions involving these mineral phases are also expected to impact the REE cycle. Evidence that Fe cycling in the Indian River Lagoon subterranean estuary plays an important role in REE cycling is further supported by the correlations between Fe and individual REEs in the sampled porewaters. For example, the correlation coefficients, r, for Fe with Nd and Gd are 0.85 and 0.59, respectively. The correlation between Fe and Nd is significant at greater than the 99% confidence level, whereas that between Fe and Gd is significant at close to the 95% confidence level. Interestingly, the HREE Yb shows only a weak relationship with Fe ($r = 0.12$), which is not statistically significant. Overall, these relationships suggest that the REE cycle is, in part, coupled to the Fe cycle in the Indian River Lagoon subterranean estuary such that REEs are likely released to solution during reductive dissolution of Fe(III) oxides/oxyhydroxides, and that the order of release follows: LREE > MREE $\geqslant$ HREE. This order of REE release is broadly consistent with the relative magnitude of the net SGD fluxes for LREEs and MREEs to the overlying lagoon waters (Table 5; Fig. 6). We note that similar preferential release of LREEs and MREEs to porewaters relative to HREEs has previously been reported during sediment diagenesis as minor phases within the sediments, such as Fe(III) oxides/oxyhydroxides, are solubilized by reducing conditions (Elderfield and Sholkovitz, 1987; Sholkovitz et al., 1989, 1992).

All of the REEs exhibit weak, inverse relationships with dissolved sulfide in Indian River Lagoon SGD, none of which are statistically significant: Nd ($r = -0.32$); Gd ($r = -0.22$); and Yb ($r = -0.32$). These relationships suggest that REEs are not strongly associated with sulfur cycling in the subterranean estuary. We interpret this as preliminary evidence that REEs are not removed from advecting SGD to the same degree as Fe(II) by precipitating Fe–sulfides at the base of the black, marine sediments within the Indian River Lagoon subterranean estuary. This is not surprising as convincing evidence currently does not exists implicating sulfide mineral formation with REE removal from marine waters (Naveau et al., 2006; also see Schijf et al., 1995; DeCarlo et al., 1998; Chaillou et al., 2006). Nevertheless, without sediment data for the REEs, we cannot unequivocally address whether REEs are also removed with precipitating metal sulfides in Indian River Lagoon sediments. Future investigations will involve examination of REE speciation in these sediments.

Consequently, the data and mass balance calculations presented here indicate that advective SGD fluxes, in combination with geochemical reactions occurring in the subterranean estuary, act in concert to deliver a substantial net flux of LREEs and MREEs to the overlying coastal waters of the Indian River Lagoon. Specifically, we suggest that hypoxic, terrestrial SGD mixes with DOC-rich, recirculating lagoon water in the Indian River Lagoon subterranean estuary, promoting reductive dissolution of Fe(III) oxides/oxyhydroxides that were precipitated within the aquifer sediments under sub-aerial conditions when sea-level was lower during the last glacial maximum (Roy et al., 2010). During the previous sea-level low-stand, REEs in percolating vadose waters were scavenged by precipitating Fe(III) oxides/oxyhydroxides that are now ubiquitous in these sediments. During the Holocene the former vadose zone was flooded as the water table rose in response to rising sea-level (Roy et al., 2010). Because LREEs and MREEs preferentially sorb to amorphous Fe(III) oxide/oxyhydroxides compared to HREEs in the presence of strong complexing ligands like carbonate ions (Quinn et al., 2006b; Tang and Johannesson, 2010), subsequent reductive dissolution of the Fe(III) oxides/oxyhydroxides releases relatively more LREEs and MREEs to the porewater of the subterranean estuary than HREEs. Upon release from the sediments, REEs form strong solution complexes with carbonate ions, with LREEs and MREEs predominantly forming $LnCO_3^+$ complexes at these pH's ($6.8 \leqslant pH \leqslant 7.4$), and the HREEs chiefly forming $Ln(CO_3)_2^-$ complexes (Fig. 5). Because amorphous Fe(III) oxides/oxyhydroxides exhibit a positive surface charge for $pH < 8$ (Dzombak and Morel, 1990), re-adsorption of negatively charged $Ln(CO_3)_2^-$ complexes of the HREEs to Fe(III) oxide/oxyhydroxides sequesters HREEs in the subterranean estuary. However, positively charged $LnCO_3^+$ complexes of LREEs and MREEs are stable in solution (Tang and Johannesson, 2005) and thus transported with advecting groundwater to overlying coastal waters. Heavy REEs also exhibit greater affinity for quartz than lighter REEs (Byrne and Kim, 1990), and hence, may be preferentially sorbed onto the predominant quartz grains that make up the Surficial Aquifer. However, this is unlikely to be significant as quartz grains within the aquifer sediments are typically coated with Fe(III) oxides/oxyhydroxides (Hartl, 2006; Roy et al., 2010). The net effect of these geochemical reactions on REE cycling in the Indian River Lagoon subterranean estuary is that of progressive flattening of the shale-normalized fractionation patterns as LREEs and MREEs are added to recirculating marine SGD, and hence the coastal lagoon waters and the HREEs are removed within the subterranean estuary.

5.3. Global implications

The global implications of SGD fluxes of REEs, and Nd in particular, to the coastal oceans await additional investigations at more sites around the world. It is important to note that owing to its shallow depth and microtidal characteristics, the Indian River Lagoon and its underlying subterranean estuary may be unique and thus not representative of coastal aquifers and subterranean estuaries in general. Nonetheless, the net flux of Nd to these coastal waters of Florida represents a previously unrecognized source of Nd to the coastal ocean that could conceivably be important to the global oceanic Nd budget. More importantly, our interpretation of the factors controlling SGD Nd fluxes implies that on glacial–interglacial time scales these fluxes could vary significantly due to changes in sea-level (Morrissey et al., 2010; Severmann et al., 2010; Roy et al., 2010). This could be complicated by SGD directly to the deep ocean along the shelf-slope break during sea-level low stands (Robb, 1984; Person et al., 2003, 2007; Cohen et al., 2010). As a result the use of Nd concentrations and isotopes in biogenic sediments as tracers of changes in ocean

circulation on these time scales (Frank, 2002; Goldstein and Hemming, 2003) may be more complex than previously thought. Clearly, additional investigations are warranted to constrain the spatial and temporal variations in SGD Nd fluxes to the coastal oceans.

6. CONCLUSIONS

Concentration variations of the REEs in porewaters collected across the freshwater–saltwater seepage face within the Indian River Lagoon subterranean estuary are too high to be explained by simple, binary mixing between terrestrial SGD and seawater. Furthermore, these high REE concentrations can not be explained by mixing of terrestrial SGD with recirculated Indian River Lagoon waters. Instead, the high REE concentrations at the seepage face point to *in situ* geochemical reactions occurring in the sediments of the subterranean estuary as an important source of REEs to SGD and hence, the overlying coastal lagoon waters. Specifically, geochemical reactions occurring within the subterranean estuary (e.g., reductive dissolution of Fe(III) oxides/oxyhydroxides) preferentially mobilize LREEs and MREEs from the subterranean estuary sediments. These trace elements form strong, positively charged carbonato complexes, $LnCO_3^+$, in solution and are subsequently advectively transported to the overlying coastal waters, accounting for a net flux of LREEs and MREEs from the subterranean estuary to the coastal lagoon waters. The net SGD flux of Nd to the overlying lagoon waters is ~7 times larger than the local effective river flux to the Indian River Lagoon. This previously unrecognized source of Nd to the coastal ocean could be important to the global oceanic Nd budget, and help to resolve the oceanic "Nd paradox" by accounting for a substantial fraction of the hypothesized missing Nd flux to the ocean.

The subterranean estuary beneath the Indian River Lagoon acts a sink for HREEs owing to their re-adsorption onto Fe(III) oxides/oxyhydroxides. Unlike the LREEs and MREEs, significant fractions of the HREEs occur in Indian River Lagoon porewaters as negatively charged dicarbonato complexes, $Ln(CO_3)_2^-$, which readily re-adsorb onto positively charged surface sites on Fe(III) oxides/oxyhydroxides that predominate in these circumneutral pH porewaters. The overall effect of these geochemical reactions on REE cycling in the Indian River Lagoon subterranean estuary is progressive flattening of the shale-normalized fractionation patterns as LREEs and MREEs are added to recirculating marine SGD, and thus the coastal lagoon waters and HREEs are sequestered within the sediments of the subterranean estuary. Future investigation will involve more extensive sampling for both analysis of REE concentrations and the Nd isotope compositions of groundwater and surface waters of the Indian River Lagoon system.

ACKNOWLEDGEMENTS

This work was supported by National Science Foundation grants OCE-0825920 to Johannesson and Burdige, EAR-0805331 to Johannesson, and EAR-0403461 to Cable and Martin, and a St. John's River Water Management District grant SG458AA to Martin and Cable. We thank D.A. Grimm who assisted with the REE analysis. The lead author wishes to thank Christopher White of Louisiana State University for a number of helpful discussions related to this project. The manuscript was improved by the comments of three anonymous reviewers as well as those of the AE, Sidney Hemming.

REFERENCES

Arsouze T., Dutay J.-C., Lacan F. and Jeandel C. (2009) Reconstructing the Nd oceanic cycle using a coupled dynamical–biogeochemical model. *Biogeosci. Discuss.* **6**, 5549–5588.

Bertram C. J. and Elderfield H. (1993) The geochemical balance of the rare earth elements and neodymium isotopes in the oceans. *Geochim. Cosmochim. Acta* **57**, 1957–1986.

Bethke C. M. (2008) *Geochemical and Biogeochemical Reaction Modeling*, second ed. Cambridge University Press, Cambridge, UK, 543p.

Burdige D. J. (2006) *The Geochemistry of Marine Sediments*. Princeton University Press, Princeton, NJ, 609p.

Burnett W. C., Bokuniewicz H., Huettel M., Moore W. S. and Taniguchi M. (2003) Groundwater and pore water inputs to the coastal zone. *Biogeochemistry* **66**, 3–33.

Byrne R. H. and Kim K.-H. (1990) Rare earth element scavenging in seawater. *Geochim. Cosmochim. Acta* **54**, 2645–2656.

Cable J. E., Martin J. B., Swarzenski P. W., Lindenberg M. K. and Steward J. (2004) Advection within shallow pore waters of a coastal lagoon, Florida. *Ground Water* **42**, 1011–1020.

Cable J. E., Martin J. B. and Jaeger J. (2006) Exonerating Bernouilli? Or evaluating the physics of seepage meter measurements in marine sediments. *Limnol. Oceanogr. Methods* **4**, 172–183.

Cable J. E., Martin J. B. and Taniguchi M. (2007) A review of submarine groundwater discharge: Biogeochemistry of leaky coastlines. In *Submarine Groundwater* (eds. I. S. Zekster, R. G. Dzhamalov and L. G. Everett). CRC Press, Boca Raton, FL, pp. 23–45.

Cai W.-J., Wang Y., Krest J. and Moore W. S. (2003) The geochemistry of dissolved inorganic carbon in a surficial groundwater aquifer in North Inlet, South Carolina, and the carbon fluxes to the coastal ocean. *Geochim. Cosmochim. Acta* **67**, 631–637.

Chaillou G., Anshultz P., Lavaux G. and Blanc G. (2006) Rare earth elements in the modern sediments of the Bay of Biscay (France). *Mar. Chem.* **100**, 39–52.

Charette M. A. (2007) Hydrologic forcing of submarine groundwater discharge: Insight from a seasonal study of radium isotopes in a groundwater-dominated salt marsh estuary. *Limnol. Oceanogr.* **52**, 230–239.

Charette M. A. and Sholkovitz E. R. (2002) Oxidative precipitation of groundwater-derived ferrous iron in the subterranean estuary of a coastal bay. *Geophys. Res. Lett.* **29**, 10. doi:10.1029/2001GL014512.

Charette M. A. and Buesseler K. O. (2004) Submarine groundwater discharge of nutrients and copper to an urban subestuary of Chesapeake Bay (Elizabeth River). *Limnol. Oceanogr.* **49**, 376–385.

Charette M. A., Sholkovitz E. R. and Hansel C. M. (2005) Trace element cycling in a subterranean estuary: Part 1. Geochemistry of the permeable sediments. *Geochim. Cosmochim. Acta* **69**, 2095–2109.

Cherrier J., Cable J. E., Martin J. B., Smith C. G. (2007). Porewater dissolved organic carbon gradients in a subterranean

estuary. *Am. Soc. Limnol. Oceanogr.*, Winter Meeting, Santa Fe, New Mexico.

Church T. M. (1996) An underground route for the water cycle. *Nature* **380**, 579–580.

Cohen D., Person M., Wang P., Gable C. W., Hutchinson D., Marksamer A., Dugan B., Kooi H., Groen K., Lizarralde D., Evans R. L., Day-Lewis F. D. and Lane, Jr., J. W. (2010) Origin and extent of fresh paleowaters on the Atlantic continental shelf, USA. *Ground Water* **48**, 143–158.

DeCarlo E. H., Wen X.-Y. and Irving M. (1998) The influence of redox reactions on the uptake of dissolved Ce by suspended Fe and Mn oxide particles. *Aquatic Geochem.* **3**, 357–389.

Duncan T. and Shaw T. J. (2003) The mobility of rare earth elements and redox sensitive elements in the groundwater/seawater mixing zone of a shallow coastal aquifer. *Aquatic Geochem.* **9**, 233–255.

Dzombak D. A. and Morel F. M. M. (1990) *Surface Complexation Modeling: Hydrous Ferric Oxide*. John Wiley and Sons, New York.

Elderfield H. and Greaves M. J. (1983) Determination of rare earth elements in sea water. In *Trace Metals in Sea Water* (eds. C. S. Wong, E. Boyle, K. W. Bruland, J. D. Burton and E. D. Goldberg). Plenum Press, New York, pp. 427–445.

Elderfield H. and Sholkovitz E. R. (1987) Rare earth elements in the pore waters of reducing nearshore sediments. *Earth Planet. Sci. Lett.* **82**, 280–288.

Elderfield H., Upstill-Goddard R. and Sholkovitz E. R. (1990) The rare earth elements in rivers, estuaries, and coastal seas and their significance to the composition of ocean waters. *Geochim. Cosmochim. Acta* **54**, 971–991.

Foster G. L., Bance D. and Prytulak J. (2007) No change in the neodymium isotope composition of deep water exported from the North Atlantic on glacial–interglacial time scales. *Geology* **35**, 37–40.

Frank M. (2002) Radiogenic isotopes: Tracers of past circulation and erosional input. *Rev. Geophys.* **40**. doi:10.1029/2000RG000094.

Frank M., Whiteley N., van de Flierdt T., Reynolds B. C. and O'Nions K. (2006) Nd and Pb isotope evolution of deep water masses in the eastern Indian Ocean during the past 33 Myr. *Chem. Geol.* **226**, 264–279.

Garrels R. M. and Thompson M. E. (1962) A chemical model for seawater at 25 °C and one atmosphere total pressure. *Am. J. Sci.* **260**, 57–66.

German C. R., Masuzama T., Greaves M. J., Elderfield H. and Edmond J. M. (1995) Dissolved rare earth elements in the Southern Ocean: Cerium oxidation and the influence of hydrography. *Geochim. Cosmochim. Acta* **59**, 1551–1558.

Goldstein S. J. and Jacobsen S. B. (1987) The Nd and Sr isotopic systematics of river-water dissolved materials. Implications for the sources of Nd and Sr in seawater. *Chem. Geol.* **66**, 245–272.

Goldstein S. L. and Hemming S. R. (2003) Long-lived isotopic tracers in oceanography, paleoceanography, and ice-sheet dynamics. *Treatise on Geochem.* **6**, 453–489.

Greaves M. J., Elderfield H. and Klinkhammer G. P. (1989) Determination of rare earth elements in natural waters by isotope-dilution mass spectrometry. *Anal. Chim. Acta* **218**, 265–280.

Hartl K. M. (2006). *Facies distribution and hydraulic conductivity of lagoonal sediments in a Holocene transgressive barrier island sequence, Indian River Lagoon, Florida*. M.S. thesis, University of Florida, Gainesville.

Jeandel C., Bishop J. K. and Zindler A. (1995) Exchange of neodymium and its isotopes between seawater and small and large particles in the Sargasso Sea. *Geochim. Cosmochim. Acta* **59**, 535–547.

Jeandel C., Thouron D. and Fiuex M. (1998) Concentrations and isotopic compositions of neodymium in the eastern Indian Ocean and Indonesian straits. *Geochim. Cosmochim. Acta* **62**, 2597–2607.

Johannesson K. H. and Lyons W. B. (1994) The rare earth element geochemistry of Mono Lake water and the importance of carbonate complexing. *Limnol. Oceanogr.* **39**, 1141–1154.

Johannesson K. H. and Burdige D. J. (2007) Balancing the global oceanic neodymium budget: Evaluating the role of groundwater. *Earth Planet. Sci. Lett.* **253**, 129–142.

Johannesson K. H., Lyons W. B., Yelken M. A., Gaudette H. E. and Stetzenbach K. J. (1996a) Geochemistry of rare-earth elements in hypersaline and dilute acidic natural terrestrial waters: Complexation behavior and middle rare-earth element enrichments. *Chem. Geol.* **133**, 125–144.

Johannesson K. H., Stetzenbach K. J., Hodge V. F. and Lyons W. B. (1996b) Rare earth element complexation behavior in circumneutral pH groundwaters: Assessing the role of carbonate and phosphate ions. *Earth Planet. Sci. Lett.* **139**, 305–319.

Johannesson K. H., Tang J., Daniels J. M., Bounds W. J. and Burdige D. J. (2004) Rare earth element concentrations and speciation in organic-rich blackwaters of the Great Dismal Swamp, Virginia, USA. *Chem. Geol.* **209**, 271–294.

Johannesson K. H., Cortés A., Ramos Leal J. A., Ramírez A. G. and Durazo J. (2005) Geochemistry of rare earth elements in groundwaters from a rhyolite aquifer, central México. In *Rare Earth Elements in Groundwater Flow Systems* (ed. K. H. Johannesson). Springer, pp. 187–222.

Kim G., Ryu J.-W., Yang H.-S. and Yun S.-T. (2005) Submarine groundwater discharge (SGD) into the Yellow Sea revealed by ^{228}Ra and ^{226}Ra isotopes: implications for global silicate fluxes. *Earth Planet. Sci. Lett.* **237**, 156–166.

Klinkhammer G., German C. R., Elderfield H., Greaves M. J. and Mitra A. (1994) Rare earth elements in hydrothermal fluids and plume particulates by inductively coupled plasma mass spectrometry. *Mar. Chem.* **45**, 170–186.

Klungness G. D. and Byrne R. H. (2000) Comparative hydrolysis behavior of the rare earth elements and yttrium: the influence of temperature and ionic strength. *Polyhedron* **19**, 99–107.

Lacan F. and Jeandel C. (2001) Tracing Papua New Guinea imprint on the Equatorial Pacific Ocean using neodymium isotopic compositions and rare earth element patterns. *Earth Planet. Sci. Lett.* **186**, 497–512.

Lacan F. and Jeandel C. (2005a) Acquisition of the neodymium isotope composition of the North Atlantic Deep Water. Geochem. *Geophys. Geosyst.* **6**(12), Q12008. doi:10.1029/2005GC000956.

Lacan F. and Jeandel C. (2005b) Neodymium isotopes as a new tool for quantifying exchange fluxes at the continent-ocean interface. *Earth Planet. Sci. Lett.* **232**, 245–257.

Lawrence M. G. and Kamber B. S. (2006) The behaviour of the rare earth elements during estuarine mixing – Revised. *Mar. Chem.* **100**, 147–161.

Lawrence M. G. and Kamber B. S. (2007) Rare earth element concentrations in the natural water reference materials (NRCC) NASS-5, CASS-4 and SLEW-3. *Geostand. Geoanal. Res.* **31**, 1–9.

Lee J. H. and Byrne R. H. (1992) Examination of comparative rare earth element complexation behavior using linear free-energy relationships. *Geochim. Cosmochim. Acta* **56**, 1127–1137.

Luo Y.-R. and Byrne R. H. (2001) Yttrium and rare earth element complexation by chloride ions at 25 °C. *J. Sol. Chem.* **30**, 837–845.

Luo Y.-R. and Byrne R. H. (2004) Carbonate complexation of yttrium and the rare earth elements in natural waters. *Geochim. Cosmochim. Acta* **68**, 691–699.

MacLeod K. G., Martin E. E. and Blair S. W. (2008) Nd isotopic excursion across Cretaceous ocean anoxic event 2 (Cenomanian–Turonian) in the tropical North Atlantic. *Geology* **36**, 811–814.

Martin J. B., Hartl K. M., Corbett D. R., Swarzenski P. W. and Cable J. E. (2003) A multilevel pore water sampler for permeable sediments. *J. Sed. Res.* **73**, 128–132.

Martin J. B., Cable J. E., Swarzenski P. W. and Lindenberg M. K. (2004) Enhanced submarine groundwater discharge from mixing of pore water and estuarine water. *Ground Water* **42**, 1000–1010.

Martin J., Cable J. and Jaeger J. (2005) *Quantification of advective benthic fluxes to the Indian River Lagoon, Florida. Final Report* (216). 32178-1429; Contract No SG458AA. Palatka, FL: St. Johns River Water Management District.

Martin J. B., Cable J. E., Jaeger J., Hartl K. and Smith C. G. (2006) Thermal and chemical evidence for rapid water exchange across the sediment-water interface by bioirrigation in the Indian River Lagoon, Florida. *Limnol. Oceanogr.* **51**, 1332–1341.

Martin J. B., Cable J. E., Smith C., Roy M. and Cherrier J. (2007) Magnitudes of submarine groundwater discharge from marine and terrestrial sources: Indian River Lagoon, Florida. *Water Resour. Res.*, **43**, W05440. doi:10.1029/2006WR005266.

Miller J. A. (1986) Hydrogeological framework of the Floridan Aquifer system in Florida and in parts of Georgia, Alabama, and South Carolina. *U.S. Geol. Surv. Prof. Pap.* 1403-B.

Millero F. J. (1992) Stability constants for the formation of rare earth inorganic complexes as a function of ionic strength. *Geochim. Cosmochim. Acta* **56**, 3123–3132.

Millero F. J. and Schreiber D. R. (1982) Use of the ion pairing model to estimate activity coefficients of the ionic components of natural waters. *Am. J. Sci.* **282**, 1508–1540.

Moore W. S. (1996) Large groundwater inputs to coastal waters revealed by ^{226}Ra enrichments. *Nature* **380**, 612–614.

Moore W. S. (1997) High fluxes of radium and barium from the mouth of the ganges-Brahmaputra River during low river discharge suggest a large groundwater source. *Earth Planet. Sci. Lett.* **150**, 141–150.

Moore W. S. (1999) The subterranean estuary: A reaction zone of groundwater and seawater. *Mar. Chem.* **65**, 111–125.

Moore W. S. (2010) The effect of submarine groundwater discharge on the ocean. *Annu. Rev. Mar. Sci.* **2**, 59–88.

Moore W. S., Sarmiento J. L. and Key R. M. (2008) Submarine groundwater discharge revealed by ^{228}Ra distribution in the upper Atlantic Ocean. *Nature Geosci.* **1**, 309–311.

Morrissey S. K., Clark J. F., Bennett M., Richardson E. and Stute M. (2010) Groundwater reorganization in the Floridan aquifer following Holocene sea-level rise. *Nature Geosci.* **3**, 683–687.

Nance W. B. and Taylor S. R. (1976) Rare earth element patterns and crustal evolution – I. Australian post-Archean rocks. *Geochim. Cosmochim. Acta* **40**, 1539–1551.

Naveau A., Monteil-Rivera F., Dumonceau J., Catalette H. and Simoni E. (2006) Sorption of Sr(II) and Eu(III) onto pyrite under different redox potential conditions. *J. Colloid Interf. Sci.* **293**, 27–35.

Nozaki Y. and Zhang J. (1995) The rare earth elements and yttrium in the coastal/offshore mixing zone of Tokyo Bay waters and the Kuroshio. In *Biogeochemical Processes and Ocean Flux in the Western Pacific* (eds. H. Sakai and Y. Nozaki). Terra Scientific Publishing, pp. 171–184.

Nozaki Y. and Alibo D. S. (2003) Importance of vertical geochemical processes in controlling the oceanic profiles of dissolved rare earth elements in the northeastern Indian Ocean. *Earth Planet. Sci. Lett.* **205**, 155–172.

Pahnke K., Goldstein S. L. and Hemming S. R. (2008) Abrupt changes in Antarctic intermediate water circulation over the past 25,000 years. *Nature Geosci.* **1**, 870–874.

Person M., Dugan B., Swenson J. B., Urbano L., Stott C., Taylor J. and Willett M. (2003) Pleistocene hydrogeology of the Atlantic continental shelf, New England. *Geol. Soc. Am. Bull.* **115**, 1324–1343.

Person M., McIntosh J., Bense V. and Remenda V. H. (2007) Pleistocene hydrology of North America: the role of ice sheets in reorganizing groundwater flow systems. *Rev. Geophys.* **45**, RG3007. doi:10.1029/2006RG000206.

Piepgras D. J. and Jacobsen S. B. (1992) The behavior of rare earth elements in seawater: Precise determination of variations in the North Pacific water column. *Geochim. Cosmochim. Acta* **56**, 1851–1862.

Piotrowski A. M., Goldstein S. L., Hemming S. R. and Faribanks R. G. (2005) Temporal relationships of carbon cycling and ocean circulation at glacial boundaries. *Science* **307**, 1933–1938.

Piotrowski A. M., Goldstein S. L., Hemming S. R., Fairbanks R. G. and Zylberberg D. R. (2008) Oscillating glacial northern and southern deep water formation from combined neodymium and carbon isotopes. *Earth Planet. Sci. Lett.* **272**, 394–405.

Pitzer K. S. (1979) Theory: Ion interaction approach. In *Activity Coefficients in Electrolyte Solutions V. 1* (ed. R. M. Pytkowicz). CRC Press, pp. 157–208.

Plummer L. N., Parkhurst D. L., Fleming G. W. and Dunkle S. A. (1989) PHRQPITZ, a computer program for geochemical calculations in brines. *U.S. Geol. Surv. Water-Resour. Invest. Rep.*, 88–4153.

Quinn K. A., Byrne R. H. and Schijf J. (2004) Comparative scavenging of yttrium and the rare earth elements in seawater: Competitive influences of solution and surface chemistry. *Aquatic Geochem.* **10**, 59–80.

Quinn K. A., Byrne R. H. and Schijf J. (2006a) Sorption of yttrium and rare earth elements by amorphous ferric hydroxide: Influence of pH and ionic strength. *Mar. Chem.* **99**, 128–150.

Quinn K. A., Byrne R. H. and Schijf J. (2006b) Sorption of yttrium and rare earth elements by amorphous ferric hydroxide: Influence of solution complexation with carbonate. *Geochim. Cosmochim. Acta* **70**, 4151–4165.

Robb J. M. (1984) Spring sapping on the lower continental slope offshore New Jersey. *Geology* **12**, 278–282.

Roy M. (2009) *Iron diagenesis in the Indian River Lagoon subterranean estuary, Florida, USA*. Ph.D. dissertation, University of Florida, Gainesville.

Roy M., Martin J. B., Cherrier J., Cable J. E. and Smith C. G. (2010) Influence of sea level rise on iron diagenesis in an east Florida subterranean estuary. *Geochim. Cosmochim. Acta* **74**, 5560–5573.

Rutberg R. L., Hemming S. R. and Goldstein S. L. (2000) Reduced North Atlantic deep water flux to the glacial Southern Ocean inferred from neodymium isotope ratios. *Nature* **405**, 935–938.

Scher H. D. and Martin E. E. (2004) Circulation in the Southern Ocean during the Paleogene inferred from neodymium isotopes. *Earth Planet. Sci. Lett.* **228**, 391–405.

Schijf J. and Byrne R. H. (1999) Determination of stability constants for the mono- and difluoro-complexes of Y and the REE, using a cation-exchange resin and ICP-MS. *Polyhedron* **18**, 2839–2844.

Schijf J. and Byrne R. H. (2004) Determination of $SO_4\beta_1$ for yttrium and the rare earth elements at $I = 0.66$ m and $t = 25$ °C – Implications for YREE solution speciation in sulfate-rich waters. *Geochim. Cosmochim. Acta* **68**, 2825–2837.

Schijf J., de Baar H. J. W. and Millero F. J. (1995) Vertical distributions and speciation of dissolved rare earth elements in the anoxic brines of Bannock Basin, eastern Mediterranean Sea. *Geochim. Cosmochim. Acta* **59**, 3285–3299.

Severmann S., MacManus J., Berelson W. M. and Hammond D. E. (2010) The continental shelf benthic iron flux and its isotope composition. *Geochim. Cosmochim. Acta* **74**, 3984–4004.

Sholkovitz E. R. (1992) Chemical evolution of rare earth elements: Fractionation between colloidal and solution phases of filtered river water. *Earth Planet. Sci. Lett.* **114**, 77–84.

Sholkovitz E. R. (1993) The geochemistry of rare earth elements in the Amazon River estuary. *Geochim. Cosmochim. Acta* **57**, 2181–2190.

Sholkovitz E. R. (1995) The aquatic geochemistry of rare earth elements in rivers and estuaries. *Aquatic Geochem.* **1**, 1–34.

Sholkovitz E. and Szymczak R. (2000) The estuarine chemistry of rare earth elements: comparison of the Amazon, Fly, Sepik and the Gulf of Papua systems Earth Planet. *Sci. Lett.* **179**, 299–309.

Sholkovitz E. R., Piepgras D. J. and Jacobsen S. B. (1989) The pore water chemistry of rare earth elements in Buzzards Bay sediment. *Geochim. Cosmochim. Acta* **53**, 2847–2856.

Sholkovitz E. R., Shaw T. J. and Schneider D. L. (1992) The geochemistry of rare earth elements in the seasonally anoxic water column and porewaters of Chesapeake Bay. *Geochim. Cosmochim. Acta* **56**, 3389–3402.

Sholkovitz E. R., Landing W. M. and Lewis B. L. (1994) Ocean particle chemistry: The fractionation of rare earth elements between suspended particles and seawater. *Geochim. Cosmochim. Acta* **58**, 1567–1579.

Siddall M., Khatiwala S., van de Flierdt T., Jones K., Goldstein S. L., Hemming S. and Anderson R. F. (2008) Towards explaining the Nd paradox using reversible scavenging in an ocean general circulation model. *Earth Planet. Sci. Lett.* **274**, 448–461.

Slomp C. P. and Van Cappellen P. (2004) Nutrient inputs to the coastal ocean through submarine groundwater discharge: controls and potential impact. *J. Hydrol.* **295**, 64–86.

Smith C. G., Cable J. E., Martin J. B. and Roy M. (2008a) Evaluating the source and seasonality of submarine groundwater using a radon-222 pore water transport model. *Earth Planet. Sci. Lett.* **273**, 312–322.

Smith C. G., Cable J. E. and Martin J. B. (2008b) Episodic high intensity mixing events in a subterranean estuary: Effects of tropical cyclones. *Limnol. Oceanogr.* **52**, 666–674.

Smith N. P. (1993) Tidal and nontidal flushing of Florida's Indian River Lagoon. *Estuaries* **16**, 739–746.

Snyder M., Tailefert M. and Ruppel C. (2004) Redox zonation at the saline-influences boundaries of a permeable surficial aquifer: Effects of physical forcing on the biogeochemical cycling of iron and manganese. *J. Hydrol.* **296**, 164–178.

Spiteri C., Regnier P., Slomp C. P. and Charette M. A. (2006) pH-Dependent iron oxide precipitation in a subterranean estuary. *J. Geochem. Explor.* **88**, 399–403.

Spiteri C., Slomp C. P., Charette M. A., Tuncay K. and Meile C. (2008) Flow and nutrient dynamics in a subterranean (Waquoit Bay, MA, USA): Field data and reactive transport modeling. *Geochim. Cosmochim. Acta* **72**, 3398–3412.

Swarzenski P. W., Orem W. H., McPherson B. F., Baskaran M. and Wan Y. (2006) Biogeochemical transport in the Loxahatchee River estuary, Florida: The role of submarine groundwater discharge. *Mar. Chem.* **101**, 248–265.

Tachikawa K., Jeandel C. and Dupré B. (1997) Distribution of rare earth elements and neodymium isotopes in settling particulate material of the tropical Atlantic Ocean (EUMELI site). *Deep-Sea Res. I* **44**, 1769–1792.

Tachikawa K., Jeandel C. and Roy-Barman M. (1999a) A new approach to Nd residence time: The role of atmospheric inputs. *Earth Planet. Sci. Lett.* **170**, 433–446.

Tachikawa K., Jeandel C., Vangriesheim A. and Dupré B. (1999b) Distribution of rare earth elements and neodymium isotopes in suspended particles of the tropical Atlantic Ocean (EUMELI site). *Deep-Sea Res. I* **46**, 733–756.

Tachikawa K., Athias V. and Jeandel C. (2003) Neodymium budget in the modern ocean and paleo-oceanographic implications. *J. Geophys. Res.* **108**, 3254. doi:10.1029/1999JC000285.

Tang J. and Johannesson K. H. (2005) Adsorption of rare earth elements onto Carrizo sand: Experimental investigations and modeling with surface complexation. *Geochim. Cosmochim. Acta* **69**, 5247–5261.

Tang J. and Johannesson K. H. (2010) Rare earth element adsorption onto Carrizo Sand: Influence of strong solution complexation. *Chem. Geol.* **279**, 120–133.

Taniguchi M., Burnett W. C., Cable J. E. and Turner J. V. (2002) Investigation of submarine groundwater discharge. *Hydrol. Process.* **16**, 2115–2129.

Testa J. M., Charette M. A., Sholkovitz E. R., Allen M. C., Rago A. and Herbold C. W. (2002) Dissolved iron cycling in the subterranean estuary of a coastal bay: Waquoit Bay, Massachusetts. *Biol. Bull.* **203**, 255–256.

von Blanckenburg F. (1999) Paleoceanography: Tracing past ocean circulation? *Science* **286**, 1862–1863.

Westerlund S. and Öhman P. (1992) Rare earth elements in the Arctic Ocean. *Deep-Sea Res.* **39**, 1613–1626.

Windom H. L., Moore W. S., Niencheski L. F. H. and Jahnke R. A. (2006) Submarine groundwater discharge: A large, previously unrecognized source of dissolved iron to the South Atlantic Ocean. *Mar. Chem.* **102**, 252–266.

Zhang J. and Nozaki Y. (1996) Rare earth elements and yttrium in seawater: ICP-MS determinations in the East Caroline, Coral Sea, and South Fiji basins of the western South Pacific Ocean. *Geochim. Cosmochim. Acta* **60**, 4631–4644.

Zhang Y., Lacan F. and Jeandel C. (2008) Dissolved rare earth elements tracing lithogenic inputs over the Kerguelen Plateau (Southern Ocean). *Deep-Sea Res. II* **55**, 638–652.

Associate editor: Sidney R. Hemming